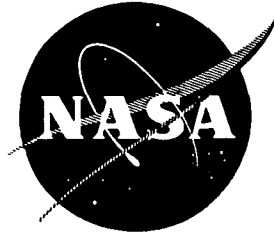


NASA CR-168305  
MRI 7014-S



**EXPERIMENTAL RESULTS FOR THE RAPID  
DETERMINATION OF THE FREEZING POINT OF FUELS**

by B. Mathiprakasam

MIDWEST RESEARCH INSTITUTE

prepared for  
NATIONAL AERONAUTICS AND SPACE ADMINISTRATION

NASA Lewis Research Center  
Contract NAS 3-22543

EXPERIMENTAL RESULTS FOR THE RAPID DETERMINATION OF  
FREEZING POINT OF FUELS

NASA Contract No. NAS3-22543  
MRI Project No. 7014-S

FINAL REPORT

February 9, 1984

Prepared by

B. Mathiprakasam  
Center for Safety and Engineering Analysis

Midwest Research Institute  
425 Volker Boulevard  
Kansas City, Missouri 64110

Prepared for

NASA - Lewis Research Center  
Cleveland, Ohio 44135

**Page intentionally left blank**

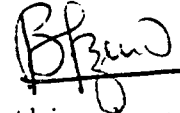
**Page intentionally left blank**

## PREFACE

This report documents the technical activities performed under the project, "Evaluation of Methods for Rapid Determination of Freezing Point of Aviation Fuels," sponsored by NASA Lewis Research Center, Cleveland. The objectives of the program were: (a) modification of the laboratory apparatus developed previously so that the test sample can be cooled to a temperature as low as  $-60^{\circ}\text{C}$  and that the rate of cooling, hold time at the end of cooling, and the rate of rewarming can be controlled; and (b) to conduct several freezing point tests on 12 fuels to study the effect of rate of cooling, hold time, and rate of rewarming.


The program was conducted in the Applied Science Section, headed by Mr. Doug Fiscus. This section is a part of the Center for Safety and Engineering Analysis, Dr. William Glauz, Director. Dr. B. Mathiprakasam, Principal Engineer, served as project leader and principal investigator, and he was assisted by Mr. William Jellison.

MIDWEST RESEARCH INSTITUTE



B. Mathiprakasam  
Principal Engineer

Approved:



W. D. Glauz, Director  
Center for Safety and  
Engineering Analysis

February 9, 1984

**Page intentionally left blank**

**Page intentionally left blank**

## TABLE OF CONTENTS

	<u>Page</u>
Summary. . . . .	1
I. Introduction . . . . .	3
II. Summary of Previous Work and Basic Analysis. . . . .	5
A. Summary of Previous Work. . . . .	5
B. Basic Analysis of the Point of Inflection Method. . . . .	6
III. Laboratory Test Apparatus. . . . .	15
A. TE Cooler . . . . .	15
B. Instrumentation and Control . . . . .	19
C. TE Cooler Characteristics . . . . .	22
IV. Experimental Data and Analysis . . . . .	31
A. The Effect of Current Flow During Rewarming and Controlled Rewarming Rate . . . . .	31
B. The Effect of Hold Time and Minimum Temperature . . . . .	33
C. The Effect of Current Flow During Cooling and Controlled Cooling Rate . . . . .	38
D. Optimum Test Procedure and Test Results . . . . .	40
V. Discussion of Test Results . . . . .	47
VI. Conclusions and Recommendations. . . . .	53
A. Conclusions . . . . .	53
B. Recommendations . . . . .	53
Appendix A - Heat Transfer Equations and Solution for the Rewarming Process . . . . .	57
References . . . . .	61

## List of Figures

<u>Figure</u>	<u>Title</u>	<u>Page</u>
1	Ideal T-t and dT/dt-t Plots for Various Substances . . . .	7
2	Experimental T-t and dT/dt-t Plots for Isooctane, Dodecane, and LFP-3. . . . .	9
3	Theoretical $\Delta T$ -t and d( $\Delta T$ )/dt-t Plots for Pure Substances.	11
4	Arrangement of Various Elements in the TE Cooler Unit. . .	16
5	Isometric View of the TE Cooler Unit . . . . .	17
6	Details of Various Elements in the TE Cooler Unit. . . . .	18
7	Temperature Control System . . . . .	20
8	Photographic View of the Laboratory Test Set-Up. . . . .	23
9	TE Cooler Characteristics in the Cooling Mode. . . . .	24
10	Current Flow During Cooling. . . . .	25
11	TE Cooler Characteristics in the Rewarming Mode. . . . .	26
12	Current Flow During Rewarming. . . . .	28
13	Current Flow During Cooling, Hold Time and Rewarming . . .	29
14	Experimental T-t and dT/dt-t Plots of LFP-1, LFP-3, and LFP-4. . . . .	43
15	Experimental T-t and dT/dt-t Plots of LFP-6, LFP-7, and LFP-8. . . . .	44
16	Experimental T-t and dT/dt-t Plots of LFP-9, LFP-14, and Fuel #7. . . . .	45
17	Experimental T-t and dT/dt-t Plots of Fuel #8, JP-5, and ERBS . . . . .	46
18	Comparison of MRI Values (Peak - 2.0°C) Versus Reported Values . . . . .	50
19	Comparison of MRI Values (Average Between Valley and Peak) Versus Reported Values . . . . .	52
20	Theoretical T-t and dT/dt-t Plots. . . . .	60

List of Tables

<u>Table</u>	<u>Title</u>	<u>Page</u>
1	Effect of Current Flow During Rewarming. . . . .	32
2	Effect of Rewarming Rate . . . . .	34
3	Effect of Hold Time. . . . .	35
4	Effect of Minimum Temperature. . . . .	37
5	Effect of Current Flow During Cooling. . . . .	39
6	Effect of Cooling Rate . . . . .	41
7	MRI Predicted Values of Tests With Optimum Test Procedure.	42
8	Reported Values of Freezing Point. . . . .	48
9	Test Results and Comparison. . . . .	49



## SUMMARY

This report documents the details of technical activities performed to develop and evaluate a rapid freezing point apparatus for fuels. The principal component of the apparatus is a thermoelectric (TE) cooler that can cool the fuel to any desired temperature up to  $-60^{\circ}\text{C}$  and can also rewarm it back to the room temperature. The concept, used to determine the freezing point, involves the identification of a point of inflection exhibited in the rewarming portion of the temperature-time curve. Theoretically it is shown that this concept is closely related to the conventional Differential Thermal Analysis (DTA). A major difference between the two is that in the method used here no reference fuel is required.

The TE cooler unit has several elements such as a sample holder, two thermoelectric modules, and two boxes containing ice-water mixture. The ice-water mixture is the medium for the TE heat sink during cooling and heat source during rewarming. DC power is applied to the cooler unit from a programmable DC power supply. The instrumentation covers the measurement of sample temperature, analog differentiation of the temperature history, analog to digital conversion of temperature and its derivative data, processing and storage of data, and printing and plotting of test results. The controls provide a variable current flow (both magnitude and direction can be varied) to the TE cooler so as to maintain any desired cooling rate, rewarming rate, and hold time between cooling and rewarming.

Experimental data were obtained on 12 different fuels by conducting several freezing point tests. In these tests, the effect of cooling rate, hold time, and rewarming rate on the measured values of freezing point was studied. Among these parameters, the rate of rewarming is found to have the most significant effect on the measured freezing point. At low rewarming rates, the results are fairly accurate but it is very difficult to identify the location of the inflection point. At high rewarming rates, the point of inflection is very distinct but the results are less accurate. The optimum rewarming rate is around  $22^{\circ}\text{C}/\text{min}$ . Hold time is found to be important only when the cooling rate near the end of cooling is very high. Also the cooling rate is found to have an insignificant effect as long as the cooling rate near the end of cooling is reasonably low ( $5^{\circ}\text{C}/\text{min}$  or less). The optimum test procedure includes cooling the sample to  $-60^{\circ}\text{C}$  with a constant current flow, providing no hold time, and finally rewarming the sample at a rate of  $22^{\circ}\text{C}/\text{min}$ .

The agreement of measured values of freezing point with those reported elsewhere is very good. It is concluded that the point of inflection method is suitable for developing portable devices to rapidly determine the freezing point of fuels.

**Page intentionally left blank**

**Page intentionally left blank**

## I. INTRODUCTION

The freezing point of aviation fuels is a key specification that defines the minimum allowable in-flight fuel temperature when the flight is operating in high, cooler altitudes. The pumpability and, consequently, the fuel system operability and safety are very much dependent on the freezing point. In the future, it is likely that the use of poorer quality petroleum and synthetic crudes will be increased as the high quality petroleum crudes become scarce and expensive. These low quality crudes would, in turn, require additional refinery processing to meet the current specifications for aviation fuels with a consequent increase in fuel cost. As a possible alternative to additional refinery processing, recent research investigations have focused on studying the consequences of relaxing the current requirements. One of the fuel specifications which is likely to be relaxed is the limit on the allowable freezing point. If this were done it is possible, under certain conditions, for the fuel temperature in the wing tank to reach or possibly go below the freezing point of the fuel. In view of this, it would be important to know the actual freezing point of the fuel at the time of delivery to the aircraft. This suggests the need for a portable freezing point apparatus for determining the fuel freezing point quickly. The currently used methods for determining the freezing point of aviation fuels are neither rapid nor suitable for field operation. In search of a suitable test method, NASA-Lewis Research Center contracted with Midwest Research Institute (MRI) to evaluate methods suitable for the rapid determination of the freezing point of aviation fuels in a field environment.

Under this contract Midwest Research Institute previously evaluated several practical methods for their suitability to determine the freezing point. Based on the evaluation process, two methods which appeared most promising were chosen for further in-depth experimental evaluation. In one of these two methods, the property of the absorption of latent heat during melting a partly frozen fuel and the consequent increase in specific heat during melting was used to detect the freezing point. The second method was based on the changes in light transmission properties that occur when a fuel melts. Our extensive experimental evaluation indicated that, in many respects, the first method, namely the thermal method, is more suitable for the development of a portable, rapid freezing point apparatus than the second, or optical method. Therefore, it was decided to choose the thermal method for freezing point determination.

Subsequently, a study was conducted to define the effect of the following parameters on the performance of the laboratory apparatus based on the thermal method:

- a. Rate at which test fuel is first cooled
- b. Minimum temperature to which the fuel is cooled
- c. Rate at which the fuel is rewarmed

From this parametric study we concluded that the freezing point of aviation fuels can be determined accurately if the fuel is cooled at a constant rate, held at the final low temperature for a finite time, and rewarmed again at a constant rate. MRI recommended to NASA that these features be incorporated into the thermal method and further tests be conducted to evaluate the suitability of this method for developing a novel, portable, rapid freezing point apparatus. Based on our recommendation, NASA granted an extension of the subject contract for an additional 12 months. Program objectives for the extension work were accordingly defined in three additional tasks.

This report contains the details of the follow on technical activities performed and the results obtained. The following 12 fuels were tested during the program: LFP-1, LFP-3, LFP-4, LFP-6, LFP-7, LFP-8, LFP-9, LFP-14, Fuel #7 and Fuel #8, JP-5, and ERBS. The reported freezing points of these fuels vary from  $-10^{\circ}$  to  $-50^{\circ}\text{C}$ .

Chapter II of this document contains a summary of technical activities performed previously and also describes the basic concept used to determine the freezing point. In Chapter III, the laboratory test apparatus used to carry out the experimental work is described, and the experimental data and analysis of the test data are presented in Chapter IV. A discussion of the results, including comparison of results obtained in this program with those reported elsewhere is provided in Chapter V. Finally, a summary of conclusions and recommendations arising from this study are presented in Chapter VI. A list of publications referenced in the report can be found in Chapter VII.

## II. SUMMARY OF PREVIOUS WORK AND BASIC ANALYSIS

In Section A of this chapter, a brief summary is presented of the technical activities previously performed. The detailed information on these technical activities is available in another report (Ref. 1). Section B contains the details of the concept analysis that was used to determine the freezing point of aviation fuels. A comparison of the Differential Thermal Analysis (DTA) method to locate the freezing point with the conceptual method is also presented.

### A. Summary of Previous Work

The first phase of this program was primarily intended to evaluate several concepts to determine the freezing point of aviation fuels and examine them for suitability to design a portable freezing point apparatus. The program objectives were: (a) the analytical evaluation and selection of practical methods to determine the freezing point of aviation fuels suitable for rapid measurement in field testing; (b) an experimental evaluation of selected methods; and (c) the design of a self-contained, portable model for rapid freezing point measurement.

To accomplish the objectives of this phase, a number of methods were evaluated to identify the more promising concepts for the development of a portable instrument to rapidly determine the freezing point of aviation fuels. The evaluation process consisted of: (a) the collection of information on the techniques employed in the past to determine the freezing point; (b) screening and selection of these techniques for their suitability in a portable unit for rapid measurement; (c) an extensive experimental evaluation of the selected techniques; and (d) the final selection of the most promising technique for design into a portable unit.

Information was obtained on several techniques and two of these were chosen for experimental evaluation. These were: (a) a thermal technique; and (b) an optical technique. The thermal method recorded the temperature difference between the sample and a nonfreezing reference fuel. The optical technique observed the change in light transmission through the sample during the phase change. A test apparatus employing these techniques was designed and built. The apparatus consisted of test and reference cells placed between thermoelectric coolers, a laser light source, an optical detector, and associated measuring instruments. An ice-water bath was used as the heat sink for the thermoelectric coolers. Both techniques gave satisfactory results for fuels, but the optical technique inexplicably failed for pure species. Because of its simplicity and superior results, the thermal method was chosen for additional tests. Further tests using the thermal method indicated that the use of a reference fuel could significantly affect the value of the measured freezing point. No solution to the problem was found. As an alternate approach, the reference fuel was eliminated, the data for the sample was digitized, and the point of inflection obtained. The temperature at the point of inflection represented the freezing point. The results using this method compared well with results obtained elsewhere by the ASTM D-2386 method and Differential Scanning Calorimetry (DSC).

A parametric study, intended to examine the effect of the rate at which the sample is cooled or rewarmed, revealed that the freezing point of aviation fuel can be determined accurately if the sample can be cooled and rewarmed under controlled conditions. The program ended with a conceptual design of a portable apparatus incorporating the point of inflection method.

## B. Basic Analysis of the Point of Inflection Method

The point of inflection method is fundamentally a thermal method. The principal difference between this conceptual method and other standard thermal methods such as DTA and DSC is that the new method does not require any reference substance. The method is referred to here as the "point of inflection" method since a point of inflection (a point where the slope of the curve attains a maximum) exhibited in the temperature-time history of a sample, being warmed from a temperature sufficiently below its freezing point, corresponds to the freezing point of the test fuel.

1. Illustration: The principles involved in the method, and the reason why there should be a point of inflection near the freezing point, is illustrated below by considering three different ideal substances. The illustrations assume that the sample was cooled/rewarmed in a TE cooler using a fixed DC current during cooling and rewarming. According to the characteristics of the TE cooler (more details of which are in Chapter III), the sample is initially cooled at a very high rate and the rate of cooling decreases as the sample cools down. During rewarming also, the sample is initially warmed at a very high rate but the rewarming rate decreases subsequently.

The expected temperature-time ( $T-t$ ) history and  $dT/dt$ -time history for the three ideal substances considered in this illustration are shown in Figure 1. A more elaborate discussion on the heat transfer equations applicable to the rewarming portions shown in this figure and also the solution of these equations can be found in Appendix A. A substance which does not freeze or melt in the temperature range of  $0^{\circ}\text{C}$  to  $-60^{\circ}\text{C}$  will exhibit  $T-t$  and  $dT/dt-t$  plots as shown in Figure 1(a). For a fixed DC current supply, the temperature of the substance will decrease exponentially as shown. Initially the absolute value of  $dT/dt$  will be very high; as the temperature is lowered, the absolute value of  $dT/dt$  will decrease. During cooling  $dT/dt$  will be negative. As soon as the magnitude and direction of the DC current is changed to provide rewarming, the sample temperature increases. At the beginning of rewarming the value of  $dT/dt$  will be very high and positive. As rewarming continues, the value of  $dT/dt$  will decrease. The apexes formed in the  $dT/dt$  curve at the beginning of cooling and at the beginning of rewarming do not represent the points of inflection but are just transitions from one mode to another. The exponential-type cooling and rewarming curves in Figure 1(a) do not exhibit any point of inflection since the test substance does not freeze or melt.

In Figure 1(b),  $T-t$  and  $dT/dt-t$  plots for a substance which freezes and melts at a fixed temperature (pure species) are shown. Here again, it is assumed that cooling and rewarming rates are not controlled.

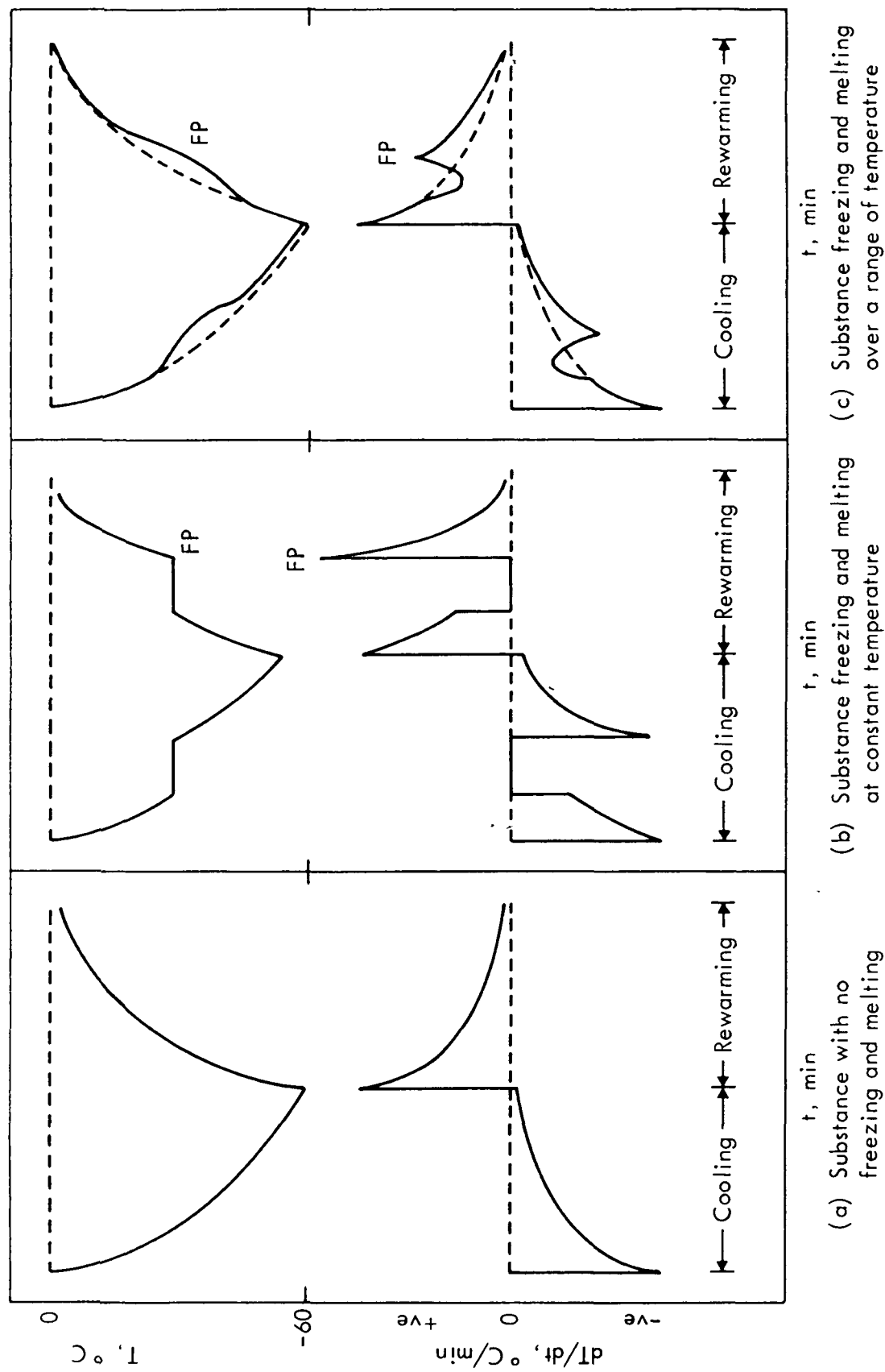


Figure 1 - Ideal  $T$ - $t$  and  $dT/dt$ - $t$  Plots for Various Substances

During cooling the value of  $dT/dt$  starts below zero and then increases in the same manner as that of a nonfreezing liquid. As soon as freezing starts  $dT/dt$  immediately becomes zero and remains zero until freezing is complete. At that point the sample is completely solid and  $dT/dt$  then drops below zero. This is the first point of inflection. It then starts to increase in a manner similar to that of a pure liquid. When the DC current is reversed, the sample starts to warm. There is a switch in  $dT/dt$  from negative to positive in a manner similar to that of a nonfreezing liquid. It then decreases until melting begins, at which time it goes directly to zero and remains there until melting is complete. At that point the sample is entirely liquid and  $dT/dt$  immediately rises to a large positive value and then decreases toward zero. The second point of inflection occurs at the peak of this rise, and corresponds to the definition of the ASTM D-2386 freezing point. It is designated "FP" in the figure.

For a substance which undergoes freezing and melting over a wide temperature range (such as aviation fuels), the  $T-t$  and  $dT/dt-t$  plots would be as shown in Figure 1(c). Here also, a fixed DC current is supplied during cooling and rewarming. In this case also, the  $dT/dt-t$  curve exhibits a point of inflection during cooling and another point of inflection during rewarming. During the freezing and melting processes, the value of  $dT/dt$  will not be zero (as in the case of pure species), since these processes are accompanied by temperature changes. The intensity of the signal exhibiting the point of inflection will also be weaker, compared to that exhibited by pure species.

The plots shown in Figure 1 are for ideal substances using an ideal cooling/rewarming device which has no thermal lag. For real substances using cooling/rewarming devices of finite thermal lag, the instantaneous changes shown in Figure 1 would take place over a finite time and the cusps of the ideal case would be rounded off.

Figure 2 shows the  $T-t$  and  $dT/dt-t$  plots obtained experimentally on isooctane, dodecane, and LFP-3, respectively. The plots for isooctane resemble those shown in Figure 1(a), since this sample does not undergo freezing or melting; clearly, there is no inflection point. The plots for dodecane resemble those shown in Figure 1(b) exhibiting a point of inflection during cooling and another point of inflection during rewarming. Plots obtained for LFP-3 are similar to those in Figure 1(c). The freezing point can be determined by noting the time (temperature) at which  $dT/dt$  attains a maximum during rewarming.

Throughout this report, we use the term "peak" to represent the point in  $dT/dt$  plot which corresponds to the point of inflection in the  $T-t$  curve. For example, the point marked "B" for dodecane and the point marked "D" for LFP-3 in Figure 2 are the peaks by this definition. We also use the term "valley" throughout this report to denote a point, preceding the peak in the  $dT/dt$  curve, where the value of  $dT/dt$  is minimum. The points marked A and C are valleys formed just before their peaks.



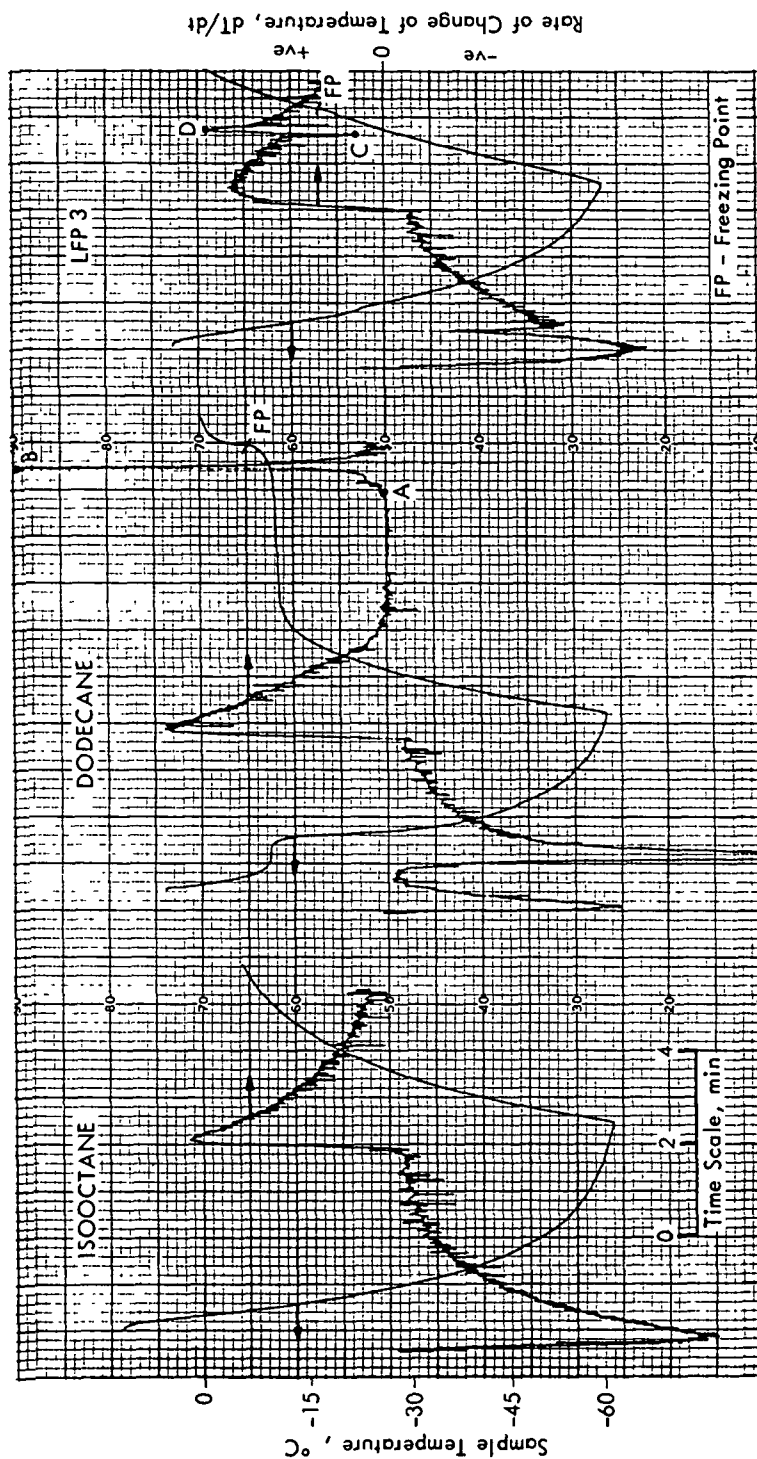


Figure 2 - Experimental T-t and dT/dt-t Plots for Isooctane, Dodecane, and LFP-3

As soon as the last few crystals are melted, during the rewarming process, the absorption of latent heat by the sample is complete, and any heat added thereafter is used solely to increase the sensible heat. Therefore, at the end of the melting process,  $dT/dt$  jumps to a high value thus forming a peak. In other words, both latent and sensible heats are absorbed before the peak, and only sensible heat is absorbed after the peak. In practice, there always exists a thermal lag, depending upon the thermal mass of the TE elements and samples. The thermal lag actually delays the time of formation of the peak. Therefore, in actual tests, the peak is formed a few seconds after crossing the freezing point. The time shift caused by the thermal lag should be kept to a minimum to accurately determine the freezing point.

A valley is formed in the  $dT/dt$  curve before the formation of the peak. A valley is a point where the absorption of latent heat is maximum during melting and therefore is a point with minimum rate of change of temperature. For pure substances,  $dT/dt$  is zero at the valley. For certain aviation fuels, the point of maximum latent heat release does not exist identifiably, and for such a case one will not be able to see a valley. The existence of a valley depends on the kind of sample being tested, whereas a peak occurs for all samples.

2. Comparison of the point of inflection and DTA methods: The similarities between the conventional DTA method and the point of inflection method can now be seen. The principles involved in a conventional DTA method are described in Reference 2. The mathematical aspects of the DTA method can also be seen elsewhere (for example, Ref. 3). Only the features that are needed to discuss the similarities between the DTA and point of inflection methods are included here.

In a DTA apparatus, the sample and a reference which does not undergo any thermal event, such as phase transition, are heated simultaneously. The heat flow is such that the rate of change of the reference temperature is constant during the experiment. Any thermal event that occurs in the sample makes the sample temperature different from the reference temperature. Such a difference in temperature ( $\Delta T$ ) indicates the presence of a thermal event in the sample. When the sample melts, the absolute value of  $\Delta T$  increases, and it attains a maximum at the end of melting. As soon as the melting process is complete, the absolute value of  $\Delta T$  decreases as the sample temperature tries to catch up to the temperature of the reference.

To see the similarities between the conventional DTA method and the conceptual point of inflection method, let us consider an illustration applicable for an ideal one-component substance. Figure 3(a) shows an idealized plot of the  $\Delta T$  curve that will be expected for an one-component substance. The base line AB is shifted from the zero  $\Delta T$  line by an amount which depends on the difference between the heat capacities of the sample and reference. At B, the process of melting begins. The sample temperature is constant during melting whereas the reference temperature increases linearly with time. Thus, the absolute value of  $\Delta T$  increases linearly, as shown by the line BC. At C, the melting process is complete; the sample which is now at a lower temperature than the reference is warmed faster, thereby de-

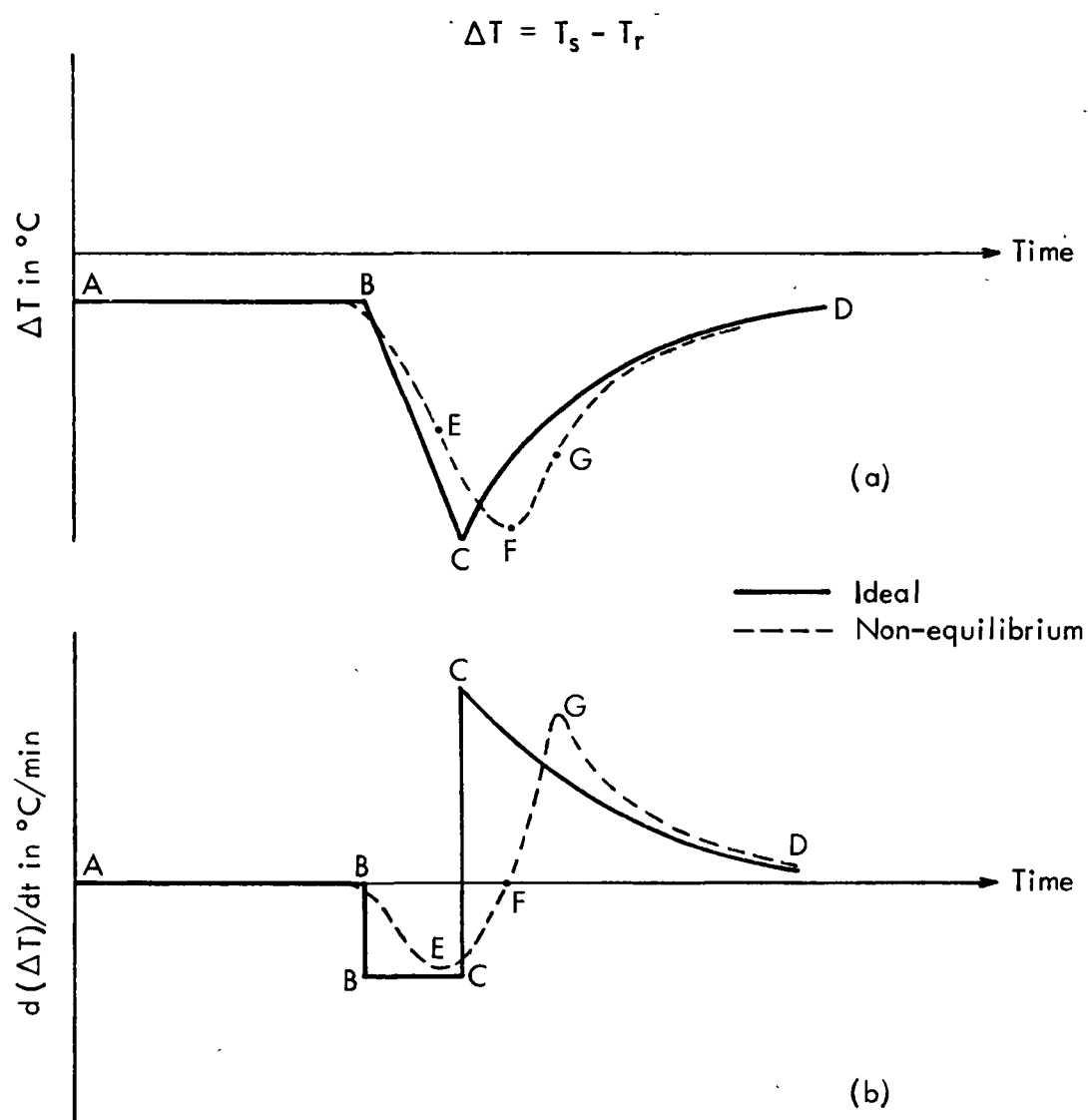


Figure 3 - Theoretical  $\Delta T$ -t and  $d(\Delta T)/dt$ -t Plots for Pure Substances

creasing the absolute value of  $\Delta T$ . Assuming that the thermal resistance between the heat source and the sample remains constant, the line CD will take an exponential form.

The  $\Delta T$  plot ABCD in Figure 3(a), can be differentiated with respect to time. The result is shown in Figure 3(b) as ABBCCD. By definition, the freezing point is the temperature at which the last crystals melt during heating the sample. In Figure 3(a), the temperature of the sample at C represents the freezing point. It is noted that a peak is formed in the  $d(\Delta T)/dt$  plot at C. Therefore, if one measures the sample temperature when the  $d(\Delta T)/dt$  plot peaks, it should correspond to the freezing point.

Now, we can show that the peak of  $d(\Delta T)/dt$  determined from the DTA method coincides in time with the peak of  $dT/dt$  obtainable from the point of inflection method. By definition,

$$\Delta T = T_s - T_r \quad (1)$$

where  $T_s$  is the sample temperature and  $T_r$  is the reference temperature, both being functions of time.  $T_r$  is controlled in a DTA apparatus, such that it is a linear function of time. Therefore, if  $T_o$  is the reference temperature at  $t=0$  (beginning of heating) and  $S$  is the heating rate in  $^{\circ}\text{C}/\text{min}$  then:

$$T_r = T_o + St \quad (2)$$

If equation (2) is used in equation (1) and then differentiated, one gets:

$$d(\Delta T)/dt = dT_s/dt - S \quad (3)$$

From equation (3), we see that the plots of  $d(\Delta T)/dt$  and  $dT/dt$  must be identical in shape except for a shift in the baseline by an amount  $S$  (recall that  $S$  is constant in time). Therefore, the time of occurrence of a peak in the  $d(\Delta T)/dt$  plot and the time of occurrence of the corresponding peak in the  $dT/dt$  plot are the same. Thus, the sample temperature measured at the peak of  $dT/dt$  should be the same as that measured at the peak of  $d(\Delta T)/dt$  and, therefore, should represent the freezing point.

The plot ABCD in Figure 3(a) and the plot ABBCCD in Figure 3(b) are theoretical plots obtainable only on an apparatus with no temperature gradients and practically negligible mass of sample. However, real apparatuses have finite temperature gradients as well as finite sample masses. The effects of these on  $\Delta T$  are shown in the dotted plot ABEFGD. We see that the cusp at B is rounded off. The point C is shifted (due to temperature gradients) to F and also is rounded off (due to the finite mass of the sample). Points of inflection occur at E and G. If this plot is differentiated the resulting plot  $d(\Delta T)/dt-t$  will look like the plot ABEFGD shown in Figure 3(b). The curve in this figure is exaggerated for illustration purposes (see Figure 2 for an actual case). This plot exhibits a valley at E and a peak at G. As discussed above, the peak of  $d(\Delta T)/dt$  will coincide with the peak of  $dT/dt$  of the point of inflection method. However, the peak of  $d(\Delta T)/dt$  (at G) does not coincide with the peak of  $\Delta T$  (which is at F). Therefore, the temperature measured at the peak of  $dT/dt$  is not the

same as the temperature at the peak of  $\Delta T$  and to that extent, the temperature at the peak of  $dT/dt$  can contribute error in the measured freezing point.

Moynihan (Ref. 4) has found that if a DSC apparatus is used to determine the freezing point of aviation fuels, the reported freezing point agrees very well if the temperature halfway down the DSC peak on the high temperature side is taken as the freezing point. This halfway point reflects very closely the point of inflection. If we assume that his predictions on DSC plots can be extended to DTA plots to determine the freezing point, then point G in Figure 3(a) appears to be the right choice to measure the freezing point rather than point F. However, our extensive tests (described later) on several fuels indicate that the sample temperature at G is always higher than the reported freezing point. Therefore, we conclude that Moynihan's predictions with the DSC method cannot be extended to the DTA method or to the point of inflection method.

3. Practical implications: While it is known that the sample temperature must be measured at F (instead of at G) to determine the freezing point, and it is possible to detect point F from a  $\Delta T$  plot with the DTA method, it is rather complex to locate F in the  $dT/dt$  plot with the point of inflection method. One approximate solution is to assume that F lies halfway between the peak G and the preceding valley E. In this case, the sample temperatures at E and G are measured and the average is taken as the freezing point. This is a very reasonable assumption to locate the position of F and thus to determine the freezing point, provided one can locate the valley at E and the peak at G in the  $dT/dt$  plot. Our freezing point tests indicate that not all the fuels exhibit an identifiable valley even though all the fuels exhibit an identifiable peak.

An alternative approach is to assume a constant difference in temperature between the points F and G. This assumption is very reasonable if the sample size and the heating rate remain the same in all the tests with various samples. The constant difference between F and G can be estimated through the results of several evaluation tests. Then, for an unknown sample, one can determine the temperature at the peak of  $dT/dt$  (i.e., at G), then subtract the established difference to arrive at the temperature at F and declare that value as the freezing point.

In our laboratory tests, we examined both alternatives. The results obtained are presented in a later chapter.

**Page intentionally left blank**

**Page intentionally left blank**

### III. LABORATORY TEST APPARATUS

In this chapter we describe the laboratory apparatus that was designed and built to conduct freezing point tests. The principal component is the thermoelectric cooler which cools and rewarms the sample during the test; its description is given in Section A. The analog and digital instruments, data acquisition accessories, and other control devices are described in Section B. Characteristics of the TE cooler and the corresponding need for the continuous adjustment of current flow to the TE modules are explained in Section C.

#### A. TE Cooler

The principal component of the laboratory apparatus is the thermoelectric cooler. The functions of the TE cooler are: (a) to cool the test fuel to a temperature of about  $-60^{\circ}\text{C}$ ; (b) to hold the minimum temperature for a predetermined period, if desired; and (c) to warm the sample to the room temperature. The sample temperature will be measured during cooling, holding, and rewarming. The design cooling rate for the unit was selected at  $12^{\circ}\text{C}/\text{min}$ , so 5 min would be required to cool the sample from  $0^{\circ}\text{C}$ . Design hold time was 2 min. Rewarming would take place for 3 min at the design rewarming rate of  $20^{\circ}\text{C}/\text{min}$ . Thus, under design conditions, a single test can be completed in 10 min time.

The general arrangement of the various parts in the TE cooler is shown schematically in Figure 4. The sample holder loaded with a test fuel and inserted into a locator is centrally placed in the cooler unit. On each side of the sample holder is a three-stage thermoelectric module. On the outside of each TE module is a box containing a mixture of ice and water. All the parts are assembled into a housing. An isometric view of the TE cooler unit is shown in Figure 5.

The functions of the various parts in the TE cooler unit are as follows:

1. TE modules: TE modules are the prime elements in the cooler unit. Each is a three-stage commercially designed and built module. Figure 6(a) shows various dimensions of each module. There are 71 thermoelectric couples (each couple is formed of a P-leg and a N-leg) in Stage 1 (this stage is in contact with the sample holder), 71 couples in Stage 2, and 127 couples in Stage 3. Each couple has a length of 3 mm in Stages 2 and 3, and 6 mm in Stage 1. Each module can lower its cold side to  $-70^{\circ}\text{C}$  if the hot side temperature can be maintained at or below  $+20^{\circ}\text{C}$  by suitable heat rejection means. The design cooling rate is 2 Watts when the cold side temperature is  $-60^{\circ}\text{C}$ . The performance of these modules was adequate for the program since the minimum temperature requirement of  $-60^{\circ}\text{C}$  is within the limits of the module.

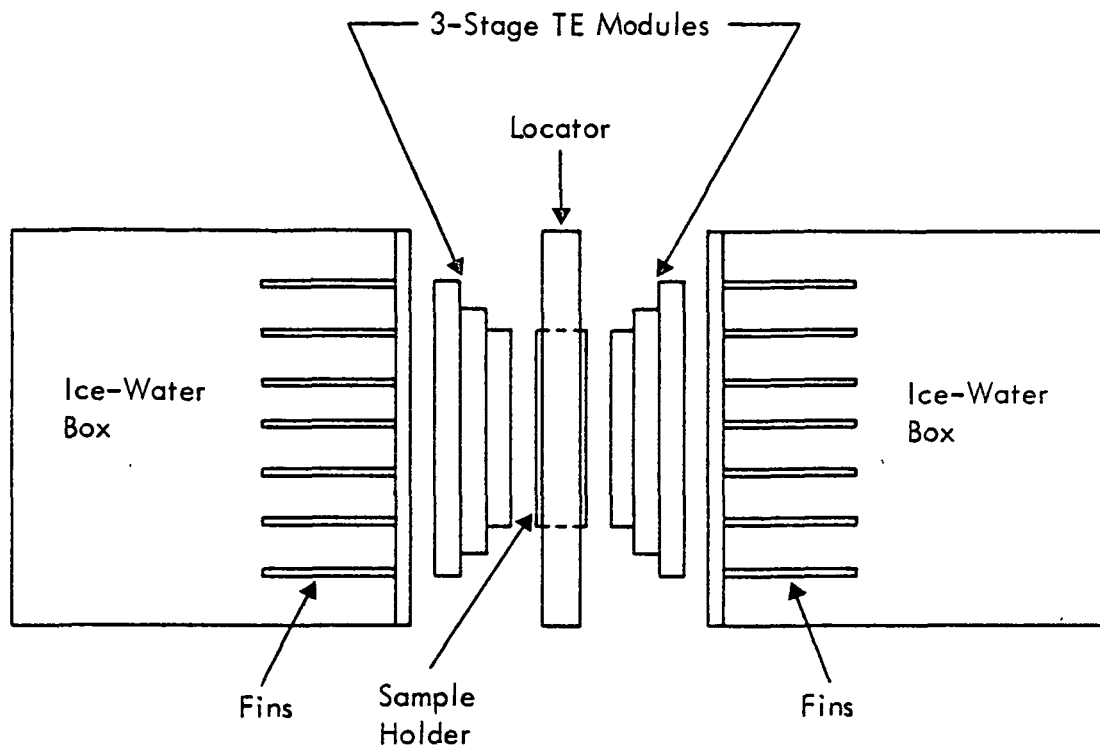


Figure 4 - Arrangement of Various Elements in the TE Cooler Unit



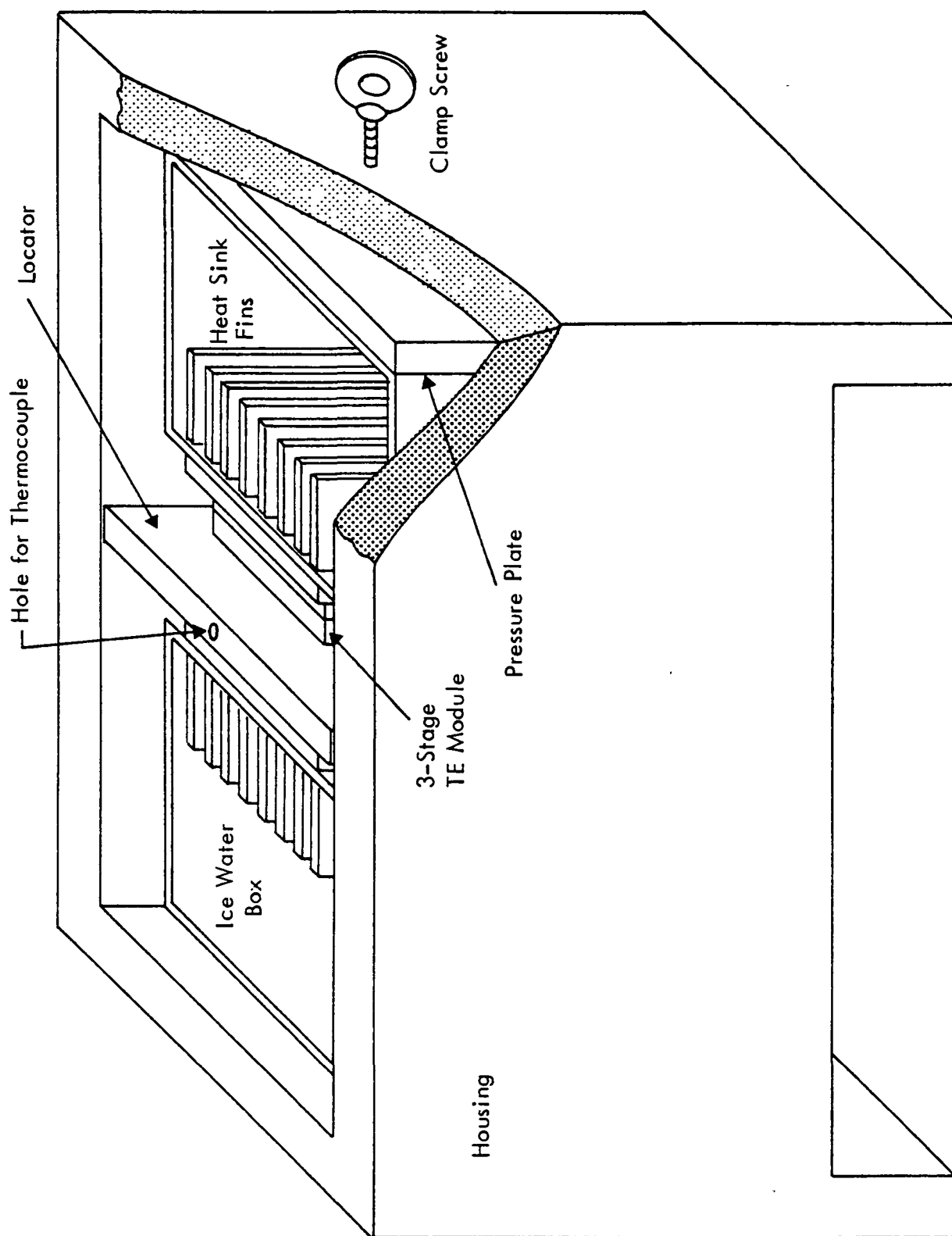


Figure 5 - Isometric View of the TE Cooler Unit

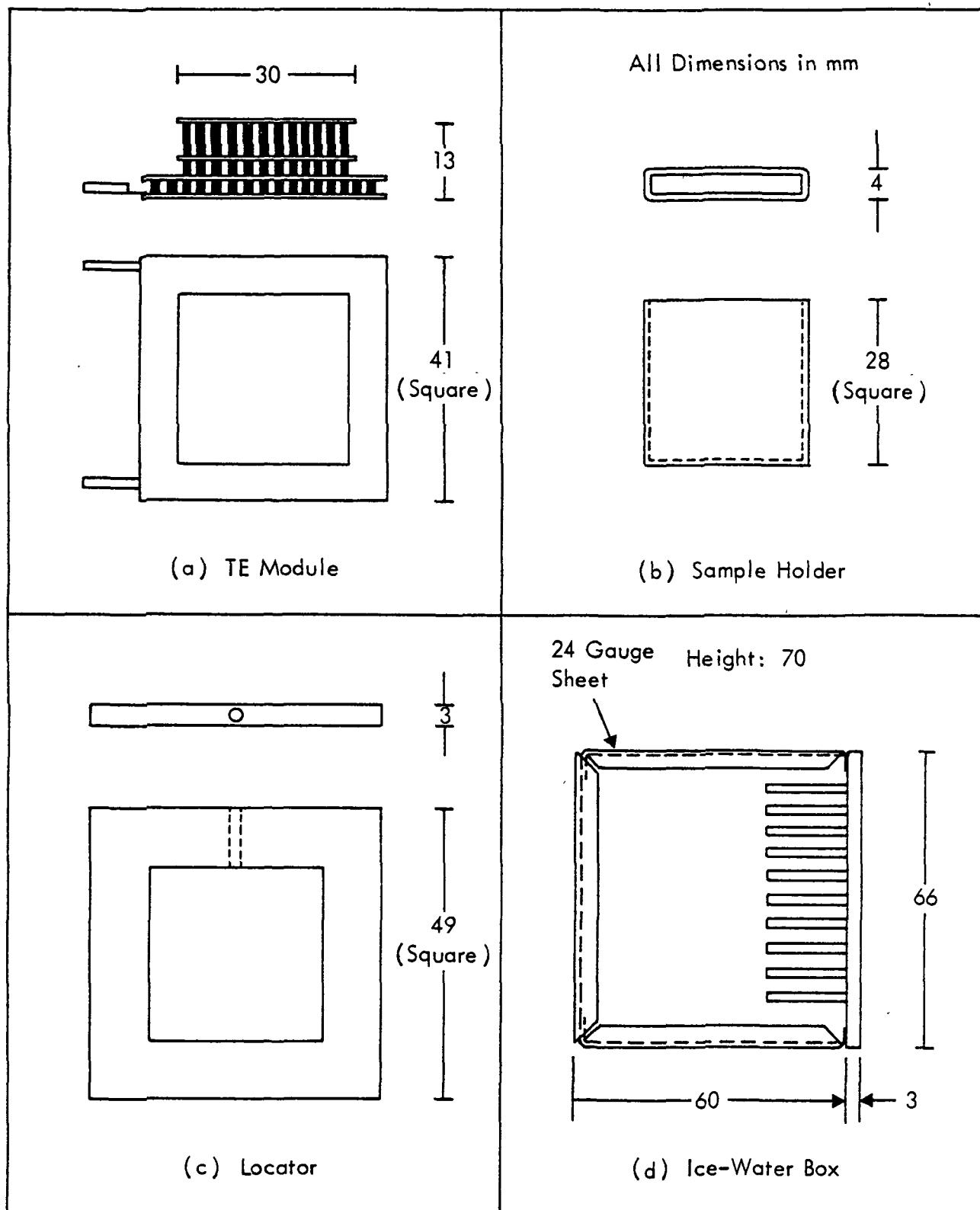


Figure 6 - Details of Various Elements in the TE Cooler Unit

2. Sample holder: The sample holder accommodates the fuel to be tested. The sketch of the sample holder is shown in Figure 6(b). The holder is 28 x 28 mm by 4 mm thick (outer dimensions). The holder is made of stainless steel sheets 0.5 mm thick. The holder can accommodate about 2.1 ml of fuel. The walls of the holder are made flat to ensure a good thermal contact with the surfaces of TE modules.

3. Locator: Placing the sample holder quickly and accurately between the TE modules was accomplished by the use of a locator as shown in Figure 6(c). A square slot in the locator accommodates the sample holder. A small hole provided in the locator top accommodates the thermocouple used to measure the temperature of the sample. The locator is made of acrylic material, 3 mm thick.

4. Ice-water box: In order to keep the temperature of the hot side of TE modules below 20°C or so, it is important to provide a heat absorbing medium on the hot side so that its bulk temperature is much less than 20°C. A mixture of ice and water was chosen as a suitable medium for this purpose. With an ice-water mixture, the bulk temperature can be maintained at 0°C, and a large amount of heat can be absorbed at 0°C (~ 334 J/g of ice). The ice-water box is designed to hold enough of the ice-water mixture at the beginning of a test. The box is approximately 63 x 66 mm size with a height of 70 mm and is shown in Figure 6(d). The front plate, to which the TE modules are soldered, is a brass heat sink having a base plate 3.2 mm thick and heat transfer fins of 25 mm length, 1.6 mm thick, and spaced at 3 fins/cm.

5. Housing: The housing is a hollow box made of 12 mm thick acrylic material. It accommodates an ice-water box and TE module assembly, one on each side, thus providing a space for inserting the locator (which carries the sample holder). The general arrangement is shown in Figure 5. The locator is held in position by tightening a clamp screw. In order to avoid the formation of dimples on the surface of the ice-water box, a pressure plate is used between the box and the clamp screw. The pressure plate also helps to distribute the point thrust of the clamp screw over the surface of the ice-water box.

## B. Instrumentation and Control

A number of components, in addition to the TE cooler, are required in the laboratory freezing point apparatus. Some of them are measuring and recording instruments, and others are control devices. The schematic arrangement of the various components in the apparatus is shown in Figure 7. The functions of the various components are as follows:

1. Electronic ice point: The temperature of the test cell is measured using a thermocouple. The thermocouple output is translated to an equivalent millivolt signal using an electronic ice point. The output signal will be 0 mv at 0°C, 0.992 mv at +25°C, and -2.152 mv at -60°C (T-type thermocouple).

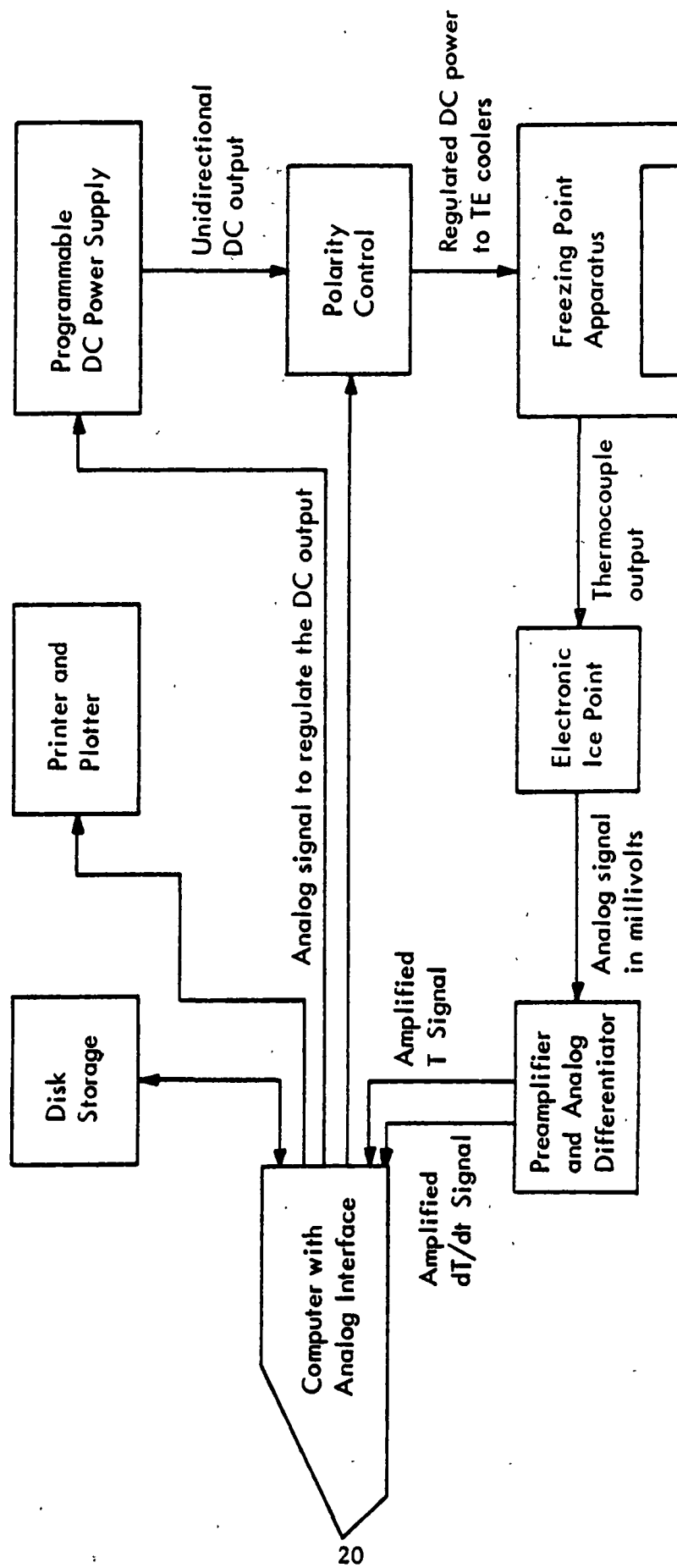


Figure 7 - Temperature Control System

2. Preamplifier and analog differentiator assembly: For the determination of the freezing point of aviation fuels we need: (a) sample temperature as a function of time; and (b) time derivative ( $dT/dt$ ) of temperature as a function of time. The preamplifier and analog differentiator assembly generate the needed information using the signal output from the electronic ice point. First, the preamplifier portion of this assembly amplifies the signal delivered from the electronic ice point by a factor of 100. In addition, the analog differentiator portion of the assembly receives the amplified temperature signal and differentiates it with respect to time. A second output from this assembly is the amplified and differentiated analog signal. Both signals are sent to the analog interface (having an A-to-D converter) installed in a computer.

3. Computer with analog interface: A microcomputer with an analog input/output interface card was used for the program. The purpose was two-fold. First, with the use of a special software program, the data such as  $T$  and  $dT/dt$  can be scanned at regular intervals (0.5 sec). For each scanning, the A to D converter receives the  $T$  and  $dT/dt$  signals in analog form, converts them to digital form, and sends them to the computer. Second, the same software generates a digital signal which is proportional to the DC current to be supplied to the cooler unit at that time. The interface card receives this digital signal and converts it to the equivalent analog signal. This information is then fed to the programmable DC power supply and polarity switching device.

4. Disk storage: The functions of the disk drive linked to the computer are to store the temperature and its derivative data and to retrieve them whenever required.

5. Printer/plotter: Upon completion of a test, the stored raw data is accessed by the software program, which produces final results. That information is sent to the printer in tabular form, and is further processed for presentation in graphic form on the same printer/plotter.

6. Programmable DC power supply: This unit supplies DC power to the thermoelectric modules. The output power is dependent on an input control voltage coming from the digital-to-analog converter (part of the computer's analog interface). Depending upon the characteristics of the TE cooler, the current flow to the TE modules has to be varied continuously during the period of a test which includes cooling, holding, and rewarming. The software determines the current flow required for a particular instant of time and generates a proportional control voltage. The programmable power supply delivers a DC current depending upon the value of the control voltage. The DC power output from the supply is always unidirectional.

7. Polarity control: In our experiments it was necessary to reverse the direction of flow of current during rewarming. The polarity control, which is basically a relay, was used in the system to perform this function. The polarity control is, again, actuated by the computer.

Figure 8 shows the laboratory apparatus. The TE cooler and other components can be seen in this photograph.

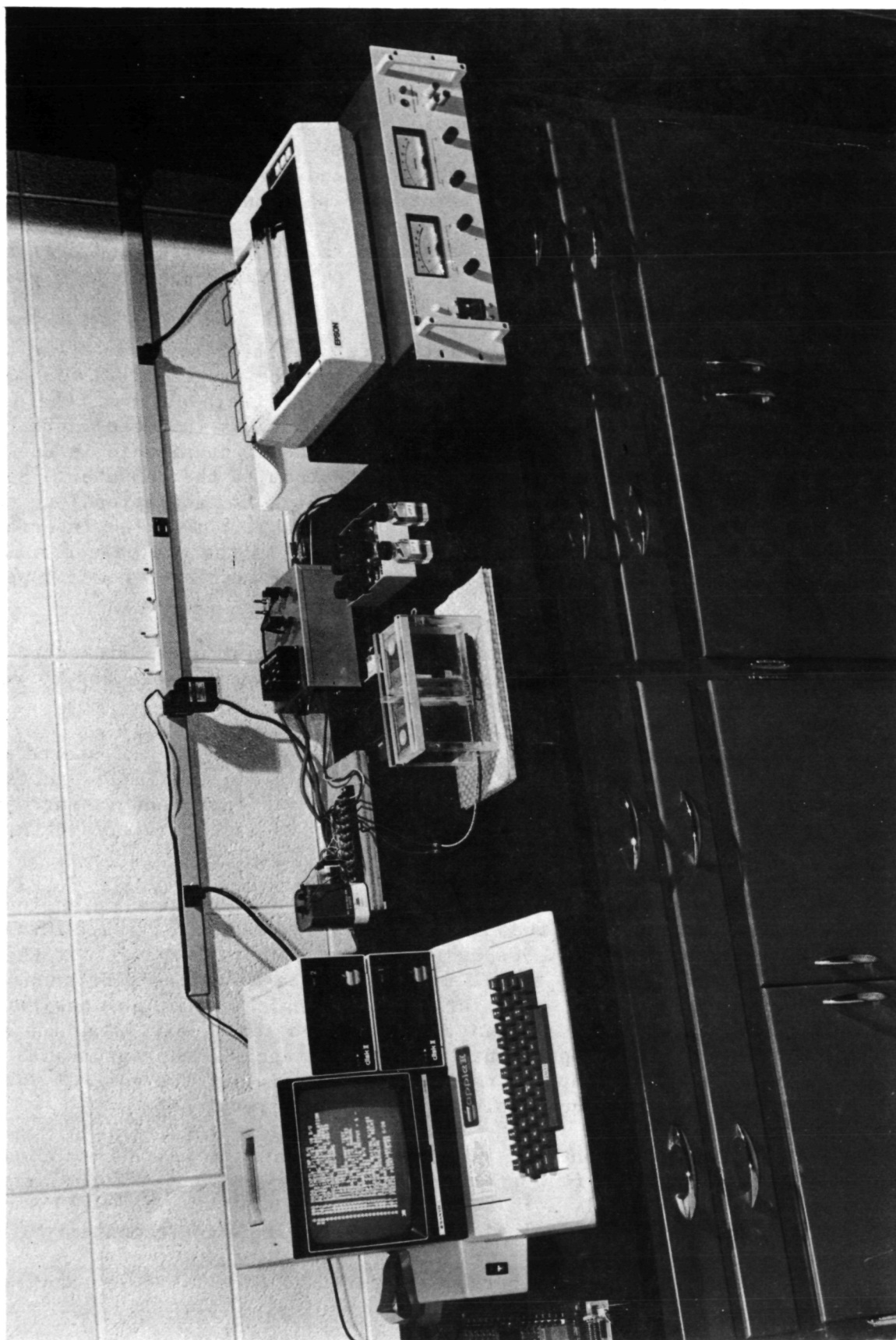


Figure 8 - Photographic View of the Laboratory Test Set-Up

### C. TE Cooler Characteristics

It is appropriate at this time to discuss some of the basic characteristics of the TE cooler unit and thus to clarify the need for varying the current flow to the TE cooler. The thermoelectric modules provided in the TE cooler operate using the principle of the Peltier Effect. When a DC voltage is applied across the TE cooler terminals, a temperature difference is generated between the two surfaces. The value of  $\Delta T$  attained under steady state conditions depends on several factors, but principally on the value of current flow. Note, however, that the unit requires a finite time to reach steady state conditions.

When a sample is cooled in the TE cooler by the application of DC power, the sample temperature decreases continuously. Initially, the sample is cooled at a very high rate but, as cooling continues, the rate of cooling decreases. Figure 9 shows the temperature-time plots obtained in our laboratory on cooling isooctane with different values of current flow to the cooler. Isooctane was chosen to study the TE cooler characteristics since it does not undergo freezing or melting in the 0 to  $-60^{\circ}\text{C}$  range. As can be seen from this figure the rate of cooling obtainable for different current flows at any instant, and the minimum temperature attainable, are different. Generally, the rate of cooling is greater with larger values of current flow; also, the minimum temperature attainable is very low at large current flow. However, there is an optimum limit of current flow beyond which any increase in current flow will actually increase the minimum attainable temperature. For the three-stage coolers used in this program, the optimum current is in the 6.5 to 7.0 amp range. The minimum attainable temperature is about  $-64^{\circ}\text{C}$ . With a current flow of 5.95 amps, isooctane can be cooled from  $0^{\circ}\text{C}$  to  $-60^{\circ}\text{C}$  in about 3 min.

If it is desired to cool a nonfreezing sample such as isooctane at a constant rate, then it is necessary to continuously adjust the current flow during cooling. The current flow as a function of time required to maintain a constant cooling rate for isooctane can be derived from the cooling curves shown in Figure 9. The results are shown in Figure 10. When isooctane is at  $0^{\circ}\text{C}$ , the current flow required for maintaining various cooling rates is below 2 amps. The required current flow increases quadratically in time thereafter. Cooling rates such as  $12^{\circ}\text{C}/\text{min}$  can be maintained for about 4.8 min, at which time the isooctane's temperature is approximately  $-57.6^{\circ}\text{C}$ . Cooling beyond this temperature cannot be maintained at  $12^{\circ}\text{C}/\text{min}$  by any current flow. Therefore the cooling rate has to decrease while approaching  $-60^{\circ}\text{C}$ .

Similarly, when a sample at  $-60^{\circ}\text{C}$  is warmed in the TE cooler, the sample temperature increases continuously. For a given current flow, the sample is initially heated at a very high rate, and as heating continues, the rate decreases. Figure 11 shows the temperature-time plots obtained in our laboratory on warming isooctane under different current flow conditions. The direction of current flow can be the same as that for cooling (with lesser magnitude) or can be reversed. Large current flow in the reversed direction provides very high heating rates. As shown in the figure, a current flow of -1.99 amps (- sign indicates that the direction is reversed) can rewarm isooctane from  $-60^{\circ}$  to  $0^{\circ}\text{C}$  in 1 min. When the current is positive, isooctane can not be warmed to  $0^{\circ}\text{C}$  and the upper limit of attainable

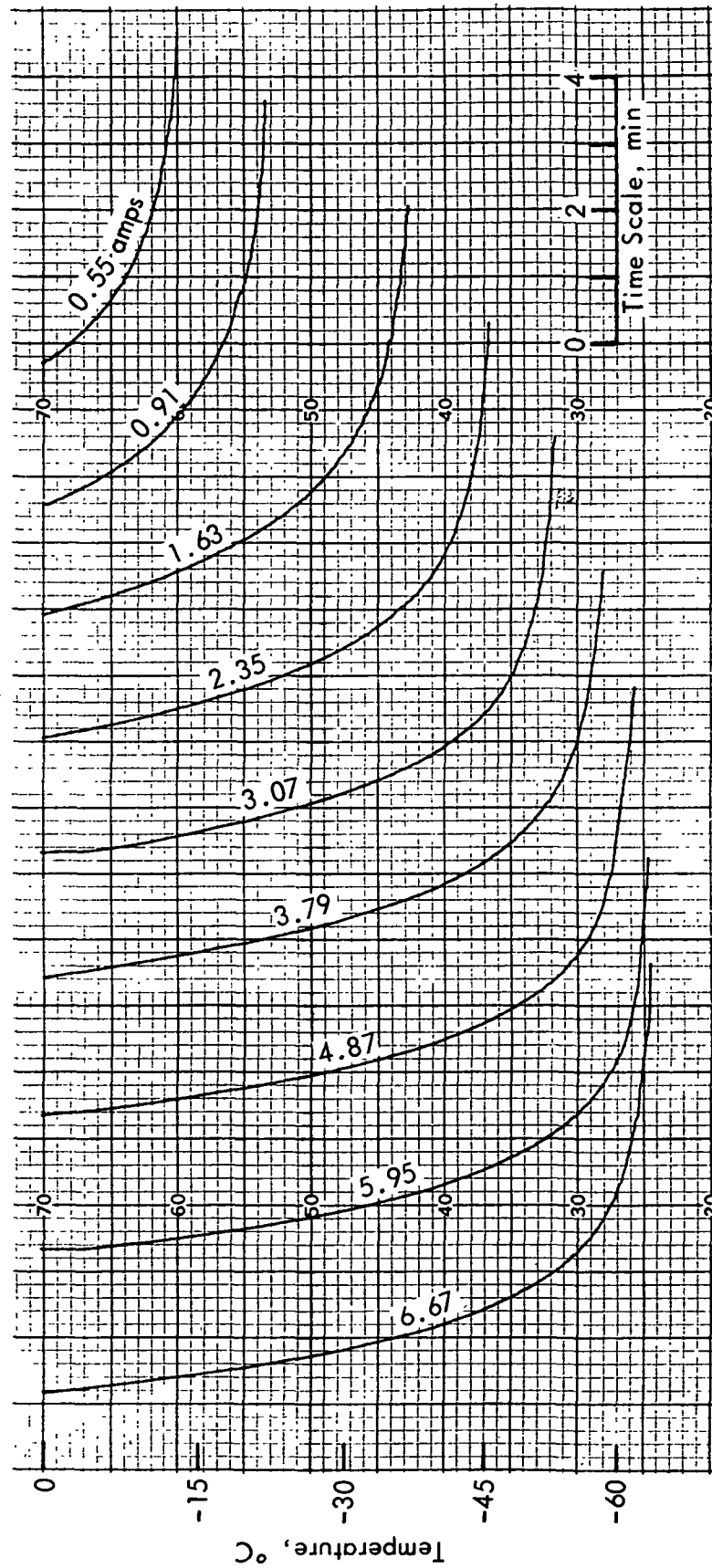


Figure 9 - TE Cooler Characteristics in the Cooling Mode



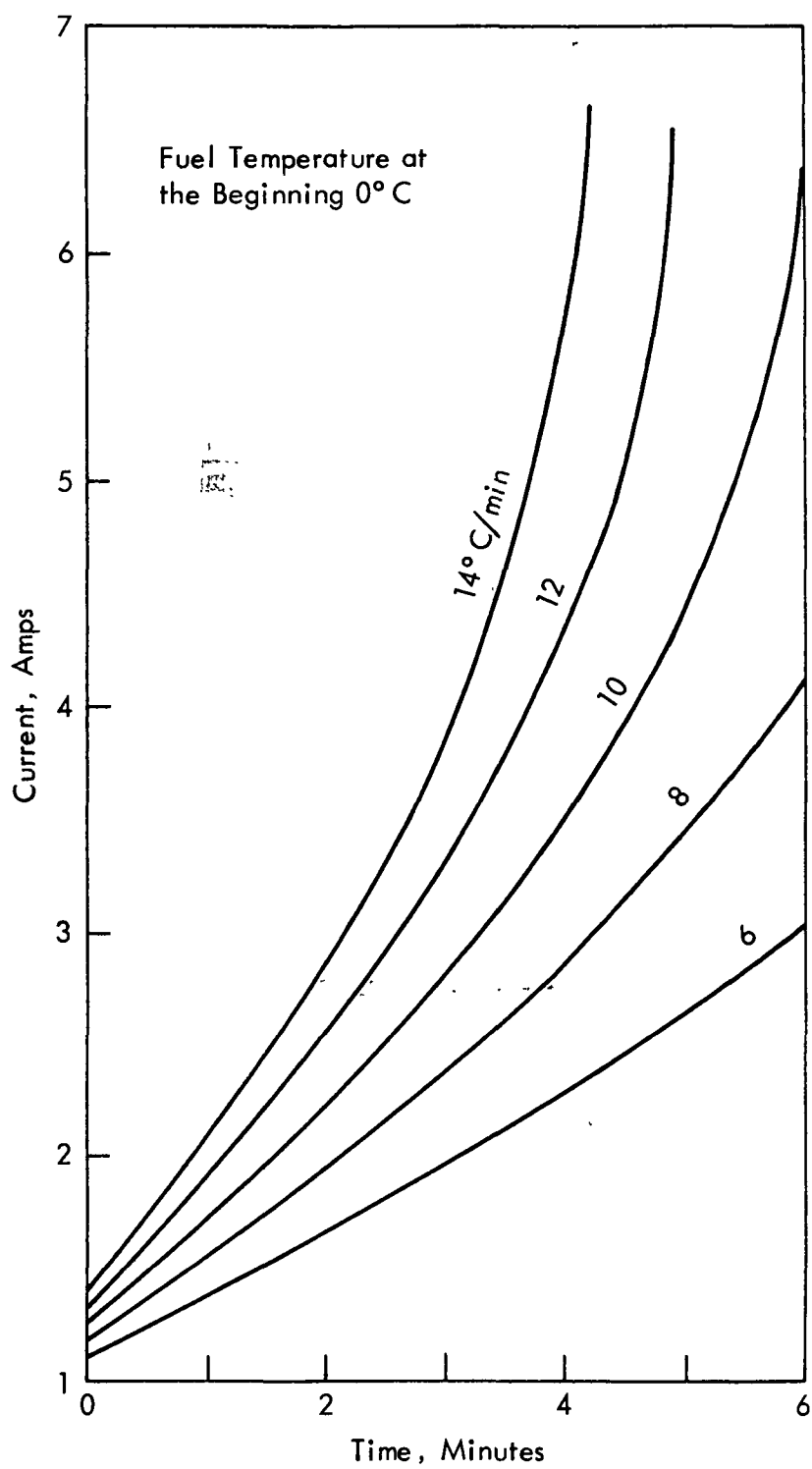


Figure 10 - Current Flow During Cooling

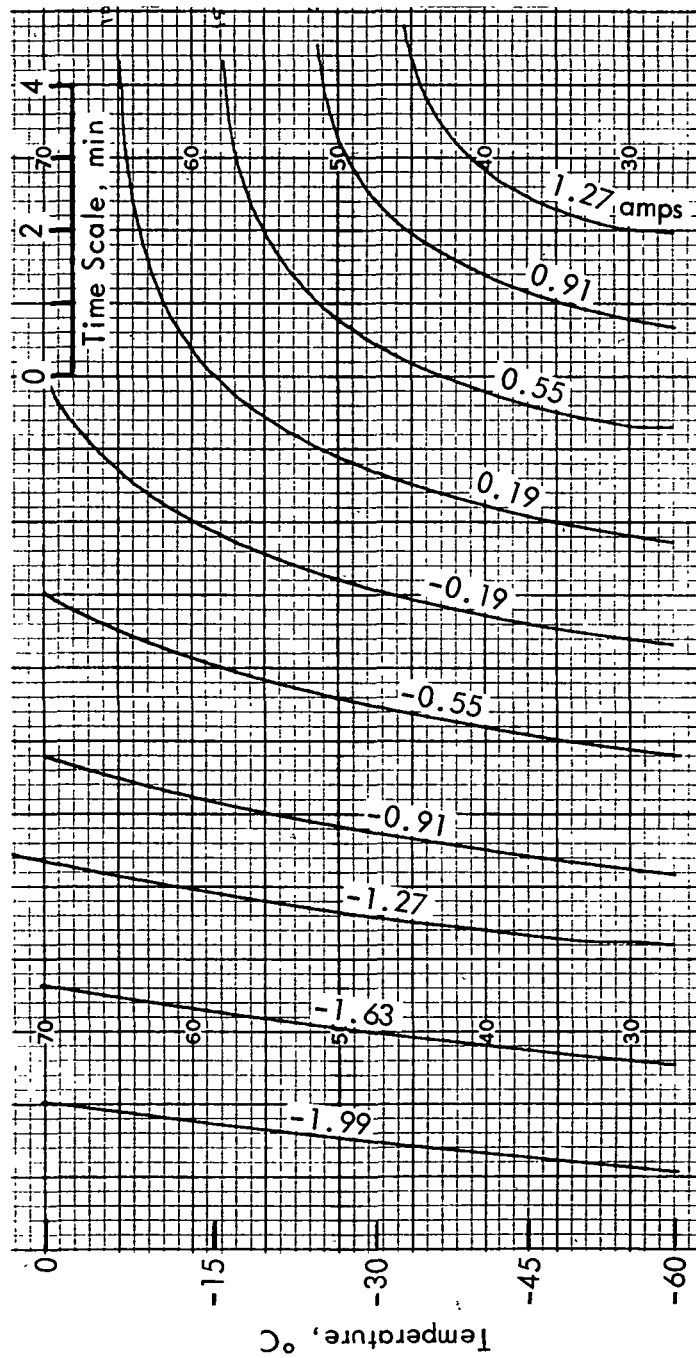


Figure 11 - TE Cooler Characteristics in the Rewarming Mode

temperature depends on the value of current flow. If it is desired to rewarm a nonfreezing sample such as isooctane at a constant rate (in  $^{\circ}\text{C}/\text{min}$ ), then it is necessary to continuously adjust the current flow. It is possible to derive the history of current flow as a function of time in order to maintain a constant rewarming rate. These results are shown in Figure 12 for isooctane. Any desired rewarming rate is possible in the temperature range  $-60^{\circ}$  to  $0^{\circ}\text{C}$ . It is also necessary to reverse the direction of current flow for any rewarming rate below  $38^{\circ}\text{C}/\text{min}$ . The relay used in the system performs this function.

Instead of isooctane, if an actual fuel sample is cooled and rewarmed in the TE cooler using the current flow histories as shown in Figures 10 and 12, the corresponding rate of cooling and rewarming obtainable will be slightly different from those obtainable for isooctane. The difference is caused by the freezing/melting behavior of the fuel sample and also by its different specific heat. In this respect, whenever a particular cooling or heating rate is referred to in the later discussions, it should be interpreted as an apparent rate which would otherwise be obtainable, had the test sample been isooctane.

In addition to maintaining constant cooling and rewarming rates, if it is desired to hold the sample temperature at the end of cooling for a short period, then the current flow to the TE modules will have to be changed during this period. Let us consider, for example, a freezing point test in which the sample is cooled at  $12^{\circ}\text{C}/\text{min}$  to  $-60^{\circ}\text{C}$ , held at  $-60^{\circ}\text{C}$  for 2 min, and then rewarmed at  $20^{\circ}\text{C}/\text{min}$ . Figure 13 shows the temperature-time history for this test. The inability to follow the  $12^{\circ}\text{C}/\text{min}$  cooling time beyond  $-57.6^{\circ}\text{C}$  (as discussed above) is not shown here for the sake of simplicity. The current history required to maintain the above described schedule is also shown in this figure. Theoretically, it would be necessary to maintain a constant current during the hold period. However, in the actual cooler, it was necessary to slowly decrease the current flow, as shown, to maintain  $-60^{\circ}\text{C}$  during that period.

During the early stages of control development, we explored the possibility of correcting any small deviation of the actual temperature from its programmed value, which may occur during a test, by appropriately raising or lowering the current flow from its programmed value. In this mode, which we called "closed control," the temperature of the sample holder (not the sample) was used as the feedback signal to quantify the correction needed in the current flow. However, our freezing point tests conducted later indicated that the oscillation of the actual temperature about the programmed value could create undesirable discontinuities in the temperature derivative when such feedback controls are used. Therefore we used the controls in their simplest form by not correcting the current flow from its programmed value (which is shown in Figure 13). We called this simple mode of control as "open control."

The software program that was used during each test, incorporates the characteristics of the TE cooler. The operator could specify a desired cooling rate, rewarming rate and hold period before beginning a test. The program is capable of generating the required current flow and a control voltage. The magnitude of this control voltage is fed to the programmable DC power supply; the sign of this control voltage is fed to the relay to condition the direction of current flow.

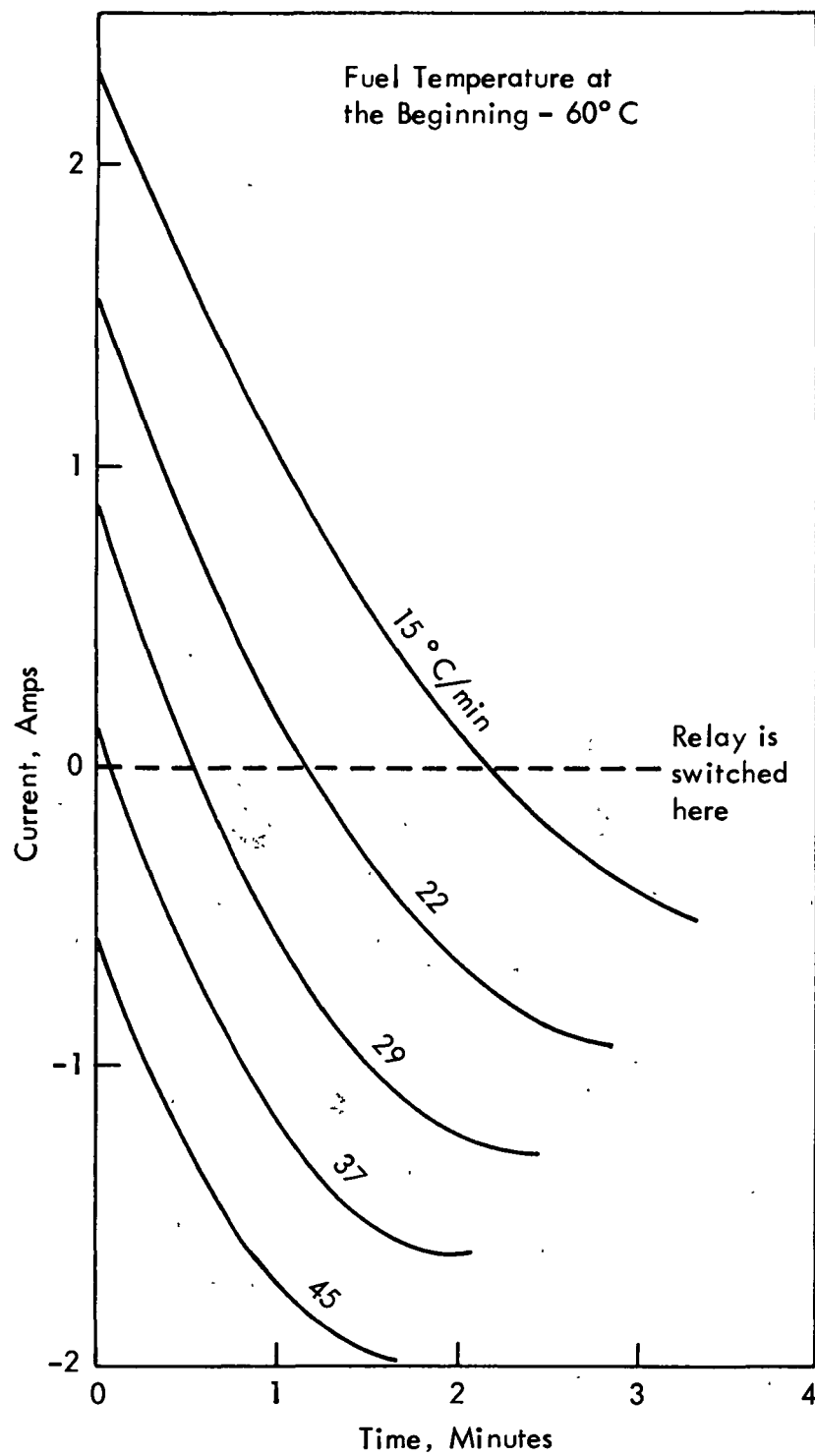


Figure 12 - Current Flow During Rewarming

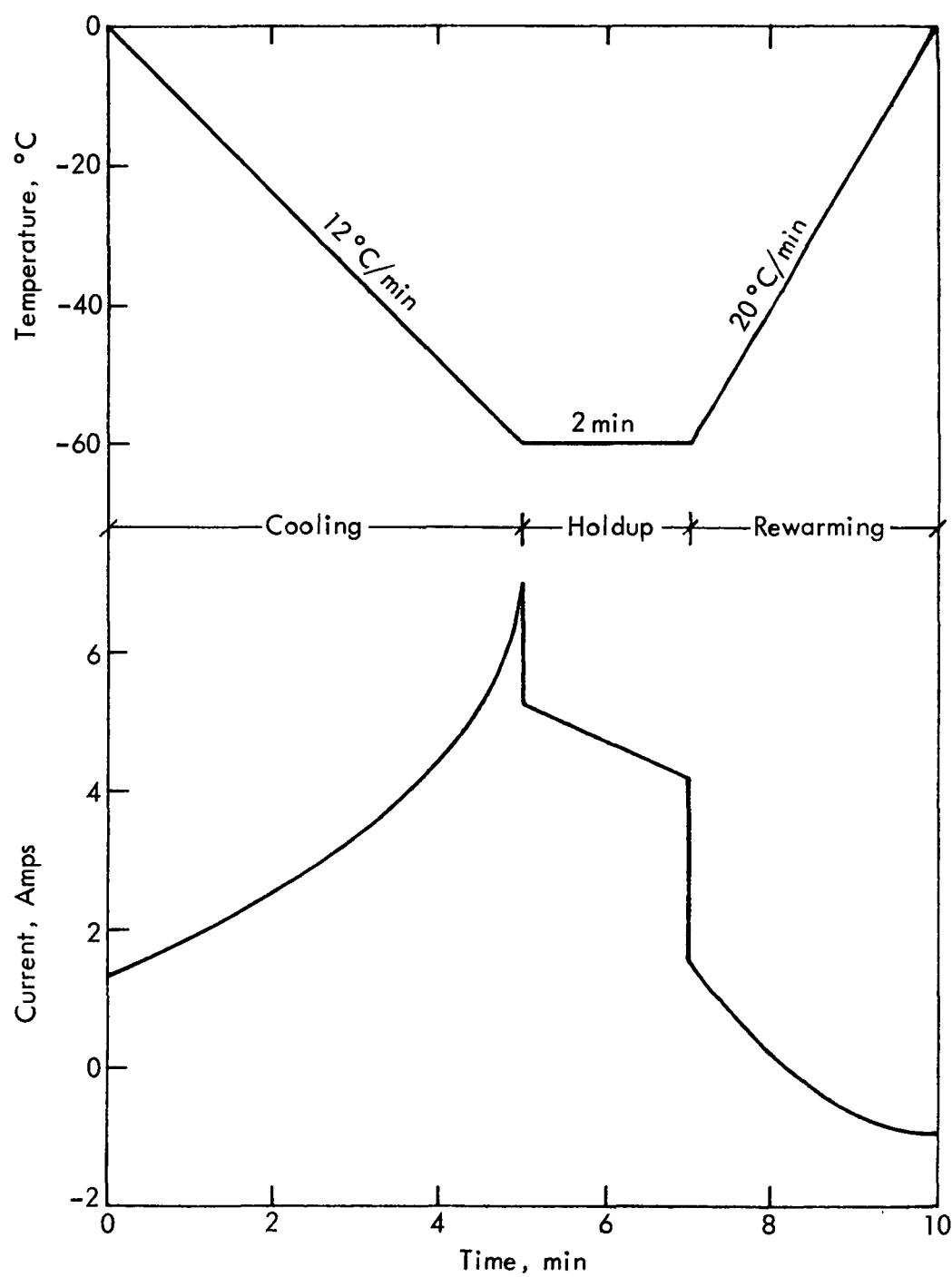


Figure 13 - Current Flow During Cooling, Hold Time, and Rewarming

**Page intentionally left blank**

**Page intentionally left blank**

#### IV. EXPERIMENTAL DATA AND ANALYSIS

In this chapter we present the data obtained on several freezing point tests. Section A contains those data from tests performed to study the effect of current flow during rewarming and the controlled rewarming rate. In Section B, the data from those tests conducted to study the effect of hold time and minimum temperature are presented. Results from varying current flow during cooling and the cooling rate appear in Section C. Based on these tests, the optimum test procedure to determine the freezing point was developed. A compilation of the data from those tests conforming to the optimum test procedure are included in Section D. This section also contains representative plots generated during the conduct of tests.

##### A. The Effect of Current Flow During Rewarming and Controlled Rewarming Rate

Several freezing point tests were conducted to study the effect of rewarming rates on the measured freezing point. These tests can be classified into two groups: (a) a series of tests in which the current flow to the TE modules was not varied (uncontrolled mode). These tests establish the effect of current flow during rewarming; and (b) other tests in which the current flow to the TE modules was varied continuously so as to provide a nearly constant rewarming rate (controlled mode). These tests were intended to study the effect of rewarming rate (in  $^{\circ}\text{C}/\text{min}$ ) on the measured values of freezing point.

Table 1 shows the results obtained on tests to study the effect of current flow during rewarming. The results presented in this table were obtained using the fuel temperature at the peak of  $dT/dt$ . In general, the effect of current flow to the TE modules during rewarming is as follows: At low rewarming current flow, the measured values of freezing point are more close to the reported values of freezing point; at higher current flow rates, the measured values are higher than the reported values. For a given current flow, the error in measured value is more for low freezing point fuels (such as LFP-8, LFP-9 and JP-5) compared to that for high freezing point fuels (such as LFP-4, LFP-7, and LFP-3). This is mainly due to the fact that, for a given current flow, the instantaneous rewarming rate in  $^{\circ}\text{C}/\text{min}$  is high for low freezing point fuels at the time of crossing the freezing point and high rewarming rates are associated with more error in the measured value. On the other hand, for the same current flow during rewarming, the instantaneous rewarming rate (in  $^{\circ}\text{C}/\text{min}$ ) is relatively low for high freezing point fuels while crossing the freezing point and this in turn minimizes the error in measured values. Therefore, a given current flow considered optimum for low freezing point fuels is not necessarily the optimum for high freezing point fuels. Therefore, it was concluded that rewarming with a supply of constant current is not a preferable choice for freezing point tests. Rewarming with a supply of varying current (and thus maintaining a constant rewarming rate) is a necessary process.

TABLE 1

EFFECT OF CURRENT FLOW DURING REWARMING  
(Freezing Point in °C)

<u>Fuel</u>	<u>(Rewarming Current in Amps (run no. shown in parenthesis))</u>				
	<u>0.19</u> <u>(6)</u>	<u>0.55</u> <u>(7)</u>	<u>0.91</u> <u>(8)</u>	<u>1.27</u> <u>(9)</u>	<u>1.63</u> <u>(10)</u>
LFP-1	-37.3	-36.2	-36.0	-31.2	-35.3
LFP-3	-16.3	-15.1	-15.7	-14.0	-14.8
LFP-4	-11.1 <sup>a</sup>	-11.0 <sup>a</sup>	-10.3	-9.1	-8.2
LFP-6	-23.9	-23.6	-26.0	-23.1	-23.8
LFP-7	-10.9	-12.1	-11.4	-9.4	-9.3
LFP-8	-48.0	-48.1	-47.5	-46.9	-37.7
LFP-9	-41.2	-41.1	-35.1	-40.6	-39.2
LFP-14	-30.7	-30.6	-29.6	-28.3	-28.3
Fuel #7	-27.0	-26.4	-25.5	-25.8	-24.9
Fuel #8	-29.4	-30.5	-29.5	-30.2	-22.8
JP-5	-45.7	-42.7	-40.7	-41.6	-38.7
ERBS	-22.9	-22.1	-21.8	-21.5	-26.9

<sup>a</sup> Required manual scanning of test data to locate the peak.



Table 2 shows the results obtained on those tests to study the effect of various rewarming rates on measured freezing point. These results were also obtained using the fuel temperature at the peak of  $dT/dt$ . The effect of rewarming the fuel at different rates can be summarized as follows. At low rewarming rates, the measured values of freezing point are more close to the reported values of freezing point; but the peak signal is very weak for some fuels and is therefore very difficult to locate its position. At high rewarming rates, the peak signal is relatively strong and is very easy to accurately locate, but the measured values are higher than the reported values of freezing point.

It was also observed that the measured freezing points of those fuels (such as JP-5 or LFP-8) which can exhibit relatively strong peak signals even at low rewarming rates are more affected when the rewarming rates are high. On the other hand, the measured freezing points of those fuels (such as LFP-4 or ERBS) which exhibit very weak peak signals at low rewarming rates are not essentially affected when the rewarming rates are high. It is suspected that fuels such as JP-5 contain a relatively large fraction of the last melting component, and therefore their behavior is more like that of pure substances. In such cases, a large amount of latent heat may be released near the freezing point, thus exhibiting strong signals even at low rewarming rates. Rewarming rates are important for such fuels, so the rates must be as low as possible. It is also suspected that some fuels, such as ERBS, contain a low fraction of the last melting component, so the amount of latent heat release for them is very low near the freezing point. The result is the exhibition of weak signals even if the rewarming rate is very high. Rewarming rates are less important for such fuels.

Based on the observations described above, it is possible to choose an optimum rewarming rate which will be suitable for nearly all the fuels. Rewarming rate must be as low as possible so as to encounter minimum error in the measured freezing point for fuels exhibiting strong peaks, and yet must be high enough to exhibit identifiable peak signals for fuels exhibiting weak peaks. From our test plots, we observed that a rewarming rate of  $15^{\circ}\text{C}/\text{min}$  was too low to exhibit reliably identifiable peak signals for LEF-4 and ERBS. A rewarming rate of  $22^{\circ}\text{C}/\text{min}$  and above was acceptable for these fuels. Therefore, we chose a rewarming rate of  $22^{\circ}\text{C}/\text{min}$  as the optimum rewarming rate.

#### B. The Effect of Hold Time and Minimum Temperature

Freezing point tests were also conducted to study the effect of allowing a finite hold time at the end of cooling. The results obtained on these tests are shown in Table 3. In these tests, the fuels were cooled to  $-60^{\circ}\text{C}$  and then held at  $-60^{\circ}\text{C}$  for a period of 0, 0.5, 1.0, 1.5, and 2.0 min before rewarming, for a total of five tests on each fuel. A rewarming rate of  $22^{\circ}\text{C}/\text{min}$  (which is the rate chosen as optimum for aviation fuels) was used during rewarming.

Our general observation is that, within the limits of repeatability attainable in our unit, the hold time at  $-60^{\circ}\text{C}$  has negligible effect on

TABLE 2

EFFECT OF REWARMING RATE  
(Freezing Point in °C)

<u>Fuel</u>	Approximate Rewarming rate in °C/min (run no. shown in parenthesis)				
	<u>15</u> <u>(11)</u>	<u>22</u> <u>(12)</u>	<u>29</u> <u>(13)</u>	<u>37</u> <u>(14)</u>	<u>45</u> <u>(15)</u>
LFP-1	-39.9	-38.9	-37.9	-37.0	-38.7
LFP-3	-17.0	-16.5	-15.5	-15.1	-18.8
LFP-4	-11.9	-12.3	-9.8	-12.1	-12.2
LFP-6	-26.2	-26.0	-26.8	-25.9	-24.2
LFP-7	-12.3	-11.0	-13.0	-9.0	-8.9
LFP-8	-49.0	-48.4	-48.3	-47.9	-37.6
LFP-9	-42.2	-42.4	-41.0	-41.2	-39.0
LFP-14	-30.1	-31.6	-30.9	-30.4	-29.5
Fuel #7	-27.5	-27.1	-26.3	-26.5	-24.7
Fuel #8	-32.0	-31.8	-31.0	-32.3	-28.5
JP-5	-46.5	-45.6	-45.4	-42.1	-40.4
ERBS	-22.5	-23.1	-21.6	-21.9	-22.4

TABLE 3

EFFECT OF HOLD TIME  
(Freezing Point in °C)

<u>Fuel</u>	<u>Hold Time in Minutes (run no. shown in parenthesis)</u>				
	<u>0.0</u> <u>(16)</u>	<u>0.5</u> <u>(17)</u>	<u>1.0</u> <u>(18)</u>	<u>1.5</u> <u>(19)</u>	<u>2.0</u> <u>(20)</u>
LFP-1	-39.1	-39.7	-38.9	-38.4	-38.5
LFP-3	-14.3	-15.1	-16.0	-15.4	-17.2
LFP-4	-11.1	-10.8	-10.9	-11.3	-10.3
LFP-6	-25.3	-25.9	-26.3	-25.3	-25.5
LFP-7	-9.8	-9.6	-12.6	-10.4	-10.6
LFP-8	-48.6	-49.1	-48.7	-48.7	-48.6
LFP-9	-42.9	-42.2	-41.7	-41.7	-40.9
LFP-14	-31.1	-31.5	-30.9	-30.7	-31.3
Fuel #7	-26.3	-26.1	-26.9	-26.1	-26.5
Fuel #8	-30.8	-31.6	-31.3	-30.5	-33.2
JP-5	-46.0	-46.0	-46.7	-46.1	-45.9
ERBS	-21.1	-21.9	-22.6	-22.3	-22.6

the measured freezing point. The purpose of providing the hold time before the commencement of rewarming is that the fuel will be able to attain thermal equilibrium at the minimum temperature. In our unit, when the fuel is cooled to  $-60^{\circ}\text{C}$ , the cooling rate achievable near this temperature is very low (around  $2^{\circ}\text{C}/\text{min}$ ) and therefore, even without having a hold time, the fuel will have negligible temperature gradients. Accordingly, any additional hold time allowed after attaining  $-60^{\circ}\text{C}$  will have very little effect on further attaining the thermal equilibrium. Therefore, we observe negligible effect on the measured freezing point.

One would then expect that if the fuel were cooled to a different temperature, say  $-30^{\circ}\text{C}$ , then the cooling rate near this temperature would be very high, the temperature gradients would also be high within the fuel at the end of cooling and therefore the hold time would be important. This expectation is satisfactorily answered in the series of tests described below.

In the next series of tests, the temperature to which the fuel was cooled before switching to rewarming was varied. Five tests were conducted on each fuel, keeping the minimum temperature as  $-20$ ,  $-30$ ,  $-40$ ,  $-50$ , and  $-60^{\circ}\text{C}$ , respectively. No hold time was allowed in all these tests. Depending upon the particular fuel being tested, a chosen minimum temperature may or may not be sufficiently below the freezing point. The freezing point was not determined if it was found that the particular minimum temperature was not sufficiently below the freezing point.

A technique that was found to work satisfactorily for all test fuels was used to first determine whether the particular minimum temperature is sufficiently below the freezing point. In this technique, the program first scanned the data of  $dT/dt$  during cooling and checked whether a peak was exhibited (showing the wax appearance point) in the cooling curve. If a peak was detected in the cooling curve, then the decision was made that the minimum temperature is sufficiently low. On the other hand, if no peak was detected in the cooling curve, then the decision is that the minimum temperature is not sufficiently lower than the freezing point.

Table 4 shows the results obtained on 60 tests conducted to study the effect of minimum temperature. For LFP-7, it was found that a minimum temperature of  $-20^{\circ}\text{C}$  is low enough to detect the freezing point, for LFP-3 and LFP-4, the minimum temperature of  $-30^{\circ}\text{C}$  is low enough; a minimum of  $-40^{\circ}\text{C}$  was low enough for LFP-6, LFP-14, Fuel #7, Fuel #8, and ERBS. LFP-1 requires a minimum temperature of  $-50^{\circ}\text{C}$  and LFP-8, LFP-9, and JP-5 require a minimum temperature of  $-60^{\circ}\text{C}$ .

The general trend observed in these tests is that the error in the measured freezing point is high at high minimum temperatures. Specifically, the measured freezing point is high if the minimum temperature attained is close to the freezing point. Weak-peak exhibiting fuels such as LFP-4 and ERBS have reverse trends. As mentioned earlier, when the minimum temperature attained is well above  $-60^{\circ}\text{C}$ , then the temperature gradients exist within the fuel at the end of cooling; and if sufficient hold time is not allowed, then this can have effect on the measured freezing point. Therefore, the conclusion is that the fuel must be cooled to  $-60^{\circ}\text{C}$  if one

TABLE 4

EFFECT OF MINIMUM TEMPERATURE  
(Freezing Point in °C)

<u>Fuel</u>	<u>Minimum Temperature in °C (run no. shown in parenthesis)</u>				
	<u>-20</u> (21)	<u>-30</u> (22)	<u>-40</u> (23)	<u>-50</u> (24)	<u>-60</u> (25)
LFP-1	-	-	-	-40.4	-37.3
LFP-3	-	-13.8	-14.8	-15.7	-16.6
LFP-4	-	-12.1	-10.1	-10.7	-9.7
LFP-6	-	-	-25.3	-26.0	-26.1
LFP-7	-9.7	-10.6	-10.0	-12.1	-9.7
LFP-8	-	-	-	-	-48.1
LFP-9	-	-	-	-	-41.5
LFP-14	-	-	-29.6	-30.8	-30.4
Fuel #7	-	-	-26.5	-25.8	-26.3
Fuel #8	-	-	-29.5	-30.4	-31.4
JP-5	-	-	-	-	-46.0
ERBS	-	-	-22.7	-21.8	-21.0

wants to eliminate the hold time or the fuel may be cooled to a temperature just below the wax appearance temperature, in which case a hold time must follow. The obvious choice is, of course, cooling to  $-60^{\circ}\text{C}$  and have zero hold time, since this requires relatively less complex software program and also many aviation fuels can be tested in this range.

### C. The Effect of Current Flow During Cooling and Controlled Cooling Rate

A number of freezing point tests were conducted to study the effect of current flow during cooling. In these studies, five tests were conducted on each fuel. The current flow to the TE modules in these five tests were 1.63, 2.71, 3.79, 4.87, and 5.95 amps, respectively. Cooling was continued until the fuel temperature reached  $-60^{\circ}\text{C}$  or a total cooling period of 5 min, whichever occurred first. On tests with current flow of 4.87 and 5.95 amps, it was possible to reach  $-60^{\circ}\text{C}$  before the 5-min cooling period. However, at 1.63 amps, the temperature attained at the end of 5 min was approximately  $-36^{\circ}\text{C}$  only. At 2.71 and 3.79 amps, the temperatures at the end of 5 min were on the order of  $-50^{\circ}$  and  $-57^{\circ}\text{C}$ , respectively. In all the cases, the rate of change of temperature at the end of the cooling was very low so that no hold time needed to be provided before starting the rewarming process. It can be recalled, from the discussions presented in Section B, that hold time is important only when the rate of cooling is significant at the end of cooling.

Fuel rewarming was done on the previously determined optimum mode of approximately  $22^{\circ}\text{C}/\text{min}$  of rewarming. Table 5 shows the results obtained in these tests. From the test results, we found in general that there was no trend in the measured freezing point as a function of current supplied during cooling. Our earlier observation was that the repeatability of test results is in most cases within  $1.5^{\circ}$  to  $2.0^{\circ}\text{C}$ . Allowing for this, we conclude that there is no effect of the cooling current on the measured freezing point.

A number of tests were also conducted to study the effect of cooling rate (in  $^{\circ}\text{C}/\text{min}$ ) on the measured values of freezing point. Again five tests were conducted on each fuel. The cooling rates used in these tests were approximately  $6^{\circ}$ ,  $8^{\circ}$ ,  $10^{\circ}$ ,  $12^{\circ}$ , and  $14^{\circ}\text{C}/\text{min}$ . A nearly constant cooling rate was achieved by continuously adjusting the current flow during cooling.

Cooling was continued until the temperature reached  $-60^{\circ}\text{C}$  or a period of 6 min elapsed, whichever was earlier. Sample temperature reached  $-60^{\circ}\text{C}$  in those tests with  $12^{\circ}$  or  $14^{\circ}\text{C}/\text{min}$  setting before 6 min. In other cooling rate settings, the actual temperature attained at the end of 6 min cooling was on the order of  $-37^{\circ}$ ,  $-48^{\circ}$ , and  $-57^{\circ}\text{C}$ , respectively, for the programmed cooling rates of  $6^{\circ}$ ,  $8^{\circ}$ , and  $10^{\circ}\text{C}/\text{min}$ . The TE cooler could not maintain the preset cooling rates when the sample temperature is below  $-55^{\circ}\text{C}$ . Therefore, in all the tests the rate of change of temperature at the end of cooling was below  $10^{\circ}\text{C}/\text{min}$ .

TABLE 5

EFFECT OF CURRENT FLOW DURING COOLING  
(Freezing Point in °C)

<u>Fuel</u>	<u>Cooling Current in Amps (run no. shown in parenthesis)</u>				
	<u>1.63</u> <u>(26)</u>	<u>2.71</u> <u>(27)</u>	<u>3.79</u> <u>(28)</u>	<u>4.87</u> <u>(29)</u>	<u>5.95</u> <u>(30)</u>
LFP-1	-	-36.5	-37.4	-38.5	-37.8
LFP-3	-14.5	-15.8	-16.3	-15.9	-15.3
LFP-4	-9.5	-10.2	-10.8	-12.2	-10.6
LFP-6	-	-27.6	-27.1	-25.2	-26.1
LFP-7	-12.2	-9.9	-9.8	-10.1	-10.2
LFP-8	-	-	-48.2	-48.3	-48.6
LFP-9	-	-	-42.1	-38.8	-41.5
LFP-14	-	-31.2	-30.3	-30.6	-30.5
Fuel #7	-24.3	-26.2	-26.2	-25.9	-25.5
Fuel #8	-	-32.6	-29.8	-32.2	-31.0
JP-5	-	-	-45.3	-45.8	-45.8
ERBS	-20.3	-21.5	-20.6	-21.1	-22.1

It was felt that this cooling rate at the end of cooling is low enough to eliminate the need for any hold time. Therefore no hold time was incorporated in the tests. Rewarming was performed again in the open control mode with approximately 22°C/min of rewarming.

Table 6 shows the results obtained in the 60 tests conducted in this way. As can be seen from this figure, there is no trend in the measured freezing point as a function of the rate of cooling. Allowing for the repeatability of test results, we conclude that there is no effect of the cooling rate on the measured freezing point.

#### D. Optimum Test Procedure and Test Results

Based on the analysis of test data presented in earlier sections, the effect of various operating parameters on the measured freezing point can be summarized as follows. The measured freezing point is a strong function of the rate at which the sample is rewarmed. For the case of aviation and diesel fuels, the optimum rewarming rate appears to be around 22°C/min. At the end of cooling, allowing a finite hold period is not required as long as the sample is cooled to a sufficiently low temperature (10-15°C below the cloud point). For the fuels tested here this was achieved by cooling all fuels to -60°C. Various cooling rates have insignificant effect on the measured freezing point. Even an uncontrolled cooling process is satisfactory for freezing point tests.

Based on the above observation, we conclude that the optimum test procedure to determine the freezing point will be as follows:

1. First cool the sample to a temperature 10-15°C below the lowest cloud point expected. Since controlled cooling is no better than uncontrolled cooling, it is advisable to choose the uncontrolled cooling process because it is simpler. Cooling to a low temperature must be done (even for testing high freezing point fuels) since it guarantees the elimination of hold time by providing a low cooling rate near the end of cooling. Also a larger number of fuels can be tested if cooled to a low temperature such as -60°C.

2. Next rewarm the sample back to room temperature. It is necessary that this heating be controlled. To do this, the current supply to the TE modules must be continuously regulated to achieve the desired constant rewarming rate. The optimum rewarming rate is approximately 22°C/min.

From among a total of 35 tests conducted on each fuel (thus making a total of 420 tests on all the fuels), five were performed as per the test procedure mentioned above. The mean and standard deviation from these tests are compiled in Table 7.

The data obtained in all the freezing point tests have been stored on floppy disks. Furthermore, at the end of each test, the temperature and its derivative were plotted. Figures 14 through 17 show representative plots obtained in the freezing point tests. Only one plot is given for each fuel, even though there are a total of 35 plots for each fuel. All these plots correspond to those tests which were performed as per the recommended test procedure described above.



TABLE 6

EFFECT OF COOLING RATE  
(Freezing Point in °C)

<u>Fuel</u>	Approximate Cooling Rate in °C/min (run no. shown in parenthesis)				
	<u>6</u> (31)	<u>8</u> (32)	<u>10</u> (33)	<u>12</u> (34)	<u>14</u> (35)
LFP-1	-	-37.3	-37.4	-37.1	-37.8
LFP-3	-14.1	-16.7	-14.5	-15.4	-14.4
LFP-4	-12.2	-11.7	-8.9	-10.2	-9.8
LFP-6	-24.2	-26.9	-27.3	-25.4	-25.4
LFP-7	-9.7	-9.6	-10.9	-9.5	-9.9
LFP-8	-	-	-48.5	-48.6	-48.6
LFP-9	-	-	-41.7	-40.7	-41.3
LFP-14	-30.0	-31.4	-30.5	-31.1	-30.8
Fuel #7	-25.1	-25.5	-25.6	-25.9	-25.7
Fuel #8	-29.3	-32.3	-30.9	-30.9	-31.6
JP-5	-	-	-44.3	-44.4	-45.6
ERBS	-21.5	-20.5	-21.0	-20.2	-20.6

TABLE 7

MRI PREDICTED VALUES OF TESTS WITH OPTIMUM TEST PROCEDURE  
(Freezing Point in °C)

<u>Fuel</u>	<u>Run No.</u>					<u>Average</u>	<u>Standard Deviation</u>
	<u>12</u>	<u>16</u>	<u>25</u>	<u>29</u>	<u>30</u>		
LFP-1	-38.9	-39.1	-37.3	-38.5	-37.8	-38.32	0.68
LFP-3	-16.5	-14.3	-16.6	-15.9	-15.3	-15.72	0.85
LFP-4	-12.3	-11.1	-9.7	-12.2	-10.6	-11.18	0.98
LFP-6	-26.0	-25.3	-26.1	-25.2	-26.1	-25.74	0.40
LFP-7	-11.0	-9.8	-9.7	-10.1	-10.2	-10.16	0.46
LFP-8	-48.4	-48.6	-48.1	-48.3	-48.6	-48.40	0.19
LFP-9	-42.4	-42.9	-41.5	-38.8	-41.5	-41.42	1.42
LFP-14	-31.6	-31.1	-30.4	-30.6	-30.5	-30.84	0.45
Fuel #7	-27.1	-26.3	-26.3	-25.9	-25.5	-26.22	0.53
Fuel #8	-31.8	-30.8	-31.4	-32.2	-31.0	-31.44	0.51
JP-5	-45.6	-46.0	-46.0	-45.8	-45.8	-45.84	0.15
ERBS	-23.1	-21.1	-21.0	-21.1	-22.1	-21.68	0.82

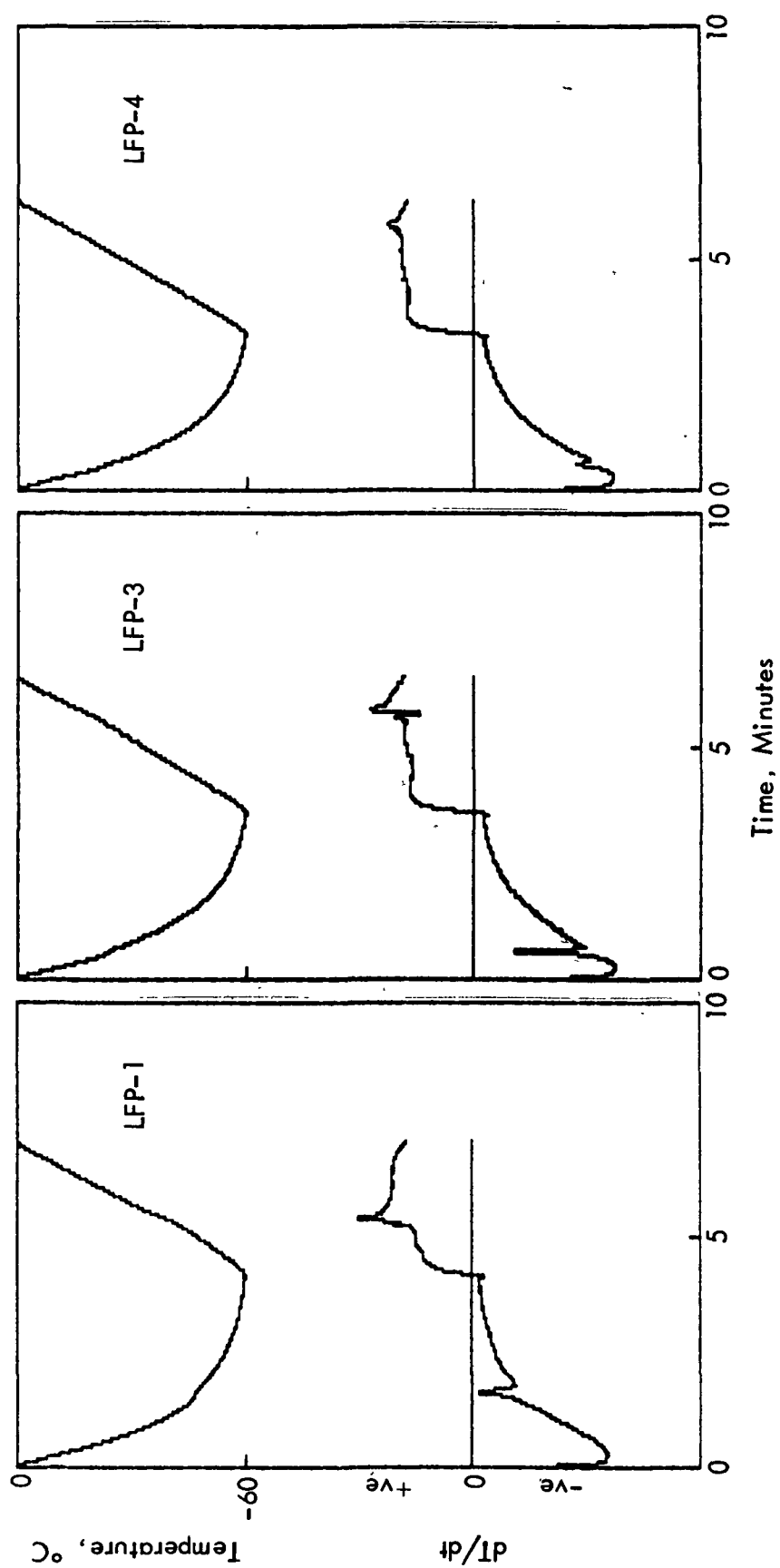


Figure 14 - Experimental T-t and dT/dt-t Plots of LFP-1, LFP-3, and LFP-4

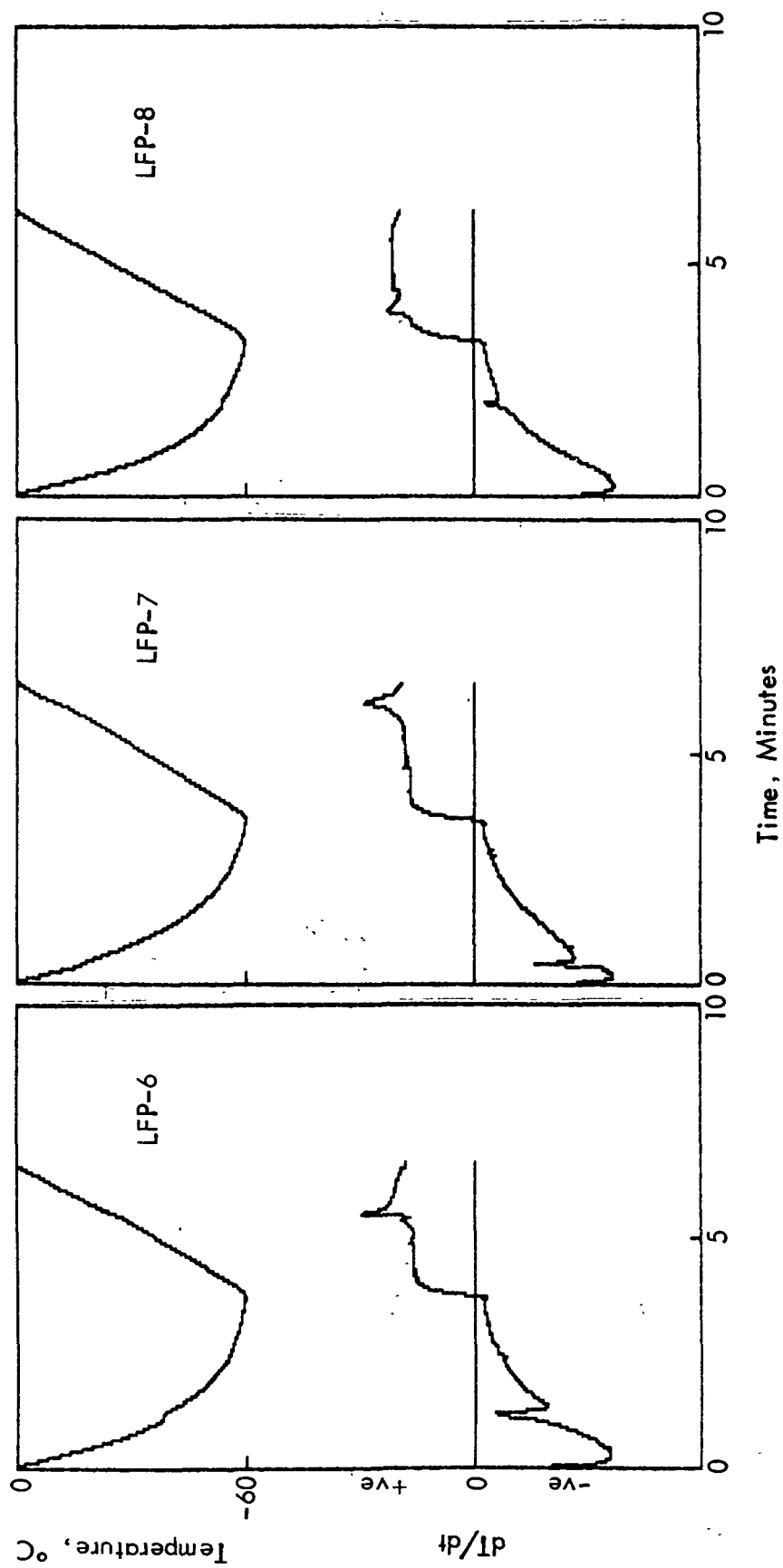


Figure 15 - Experimental T-t and dT/dt-t Plots of LFP-6, LFP-7, and LFP-8

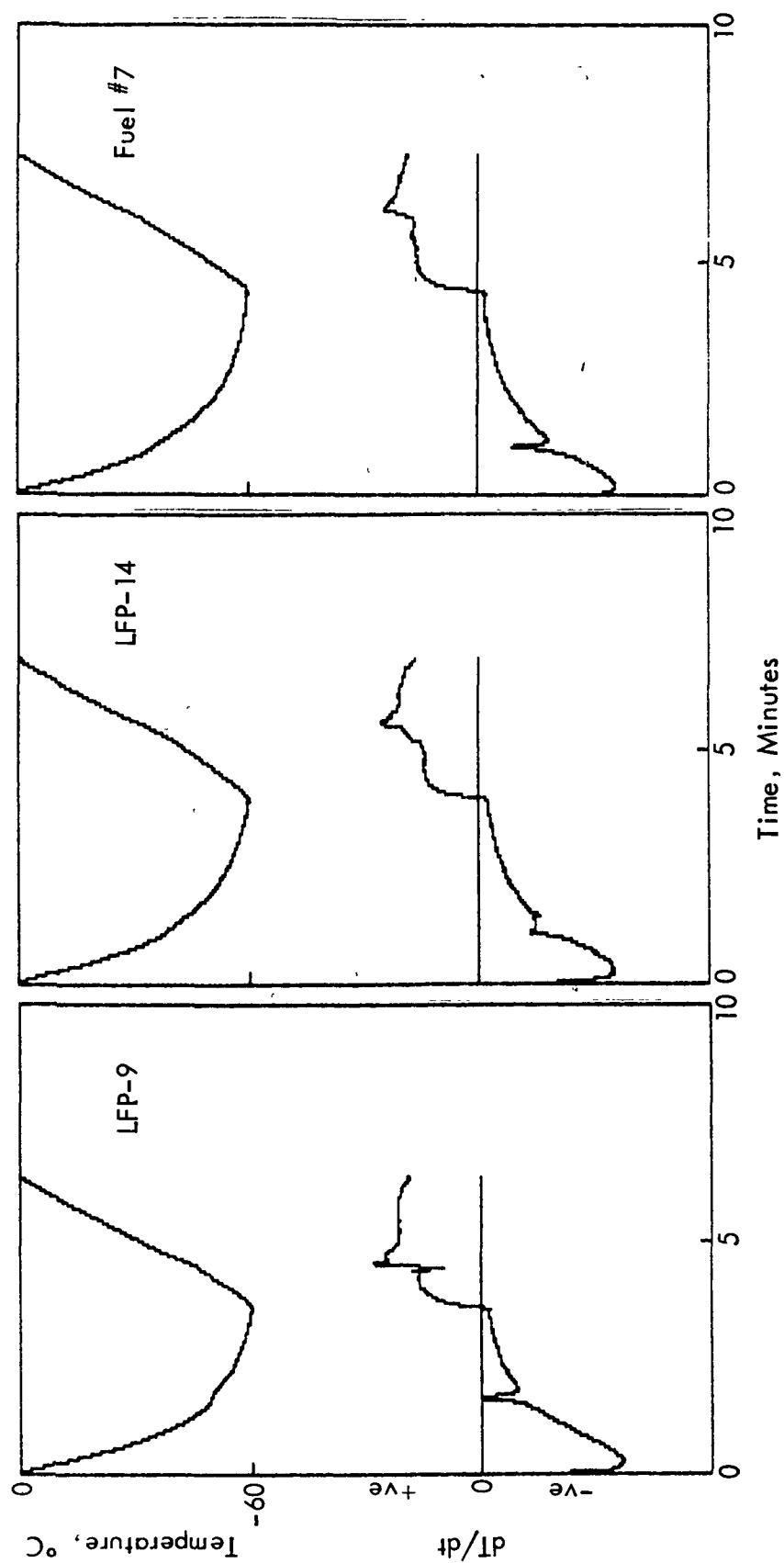


Figure 16 - Experimental T-t and  $dT/dt$ -t Plots of LFP-9, LFP-14, and Fuel #7

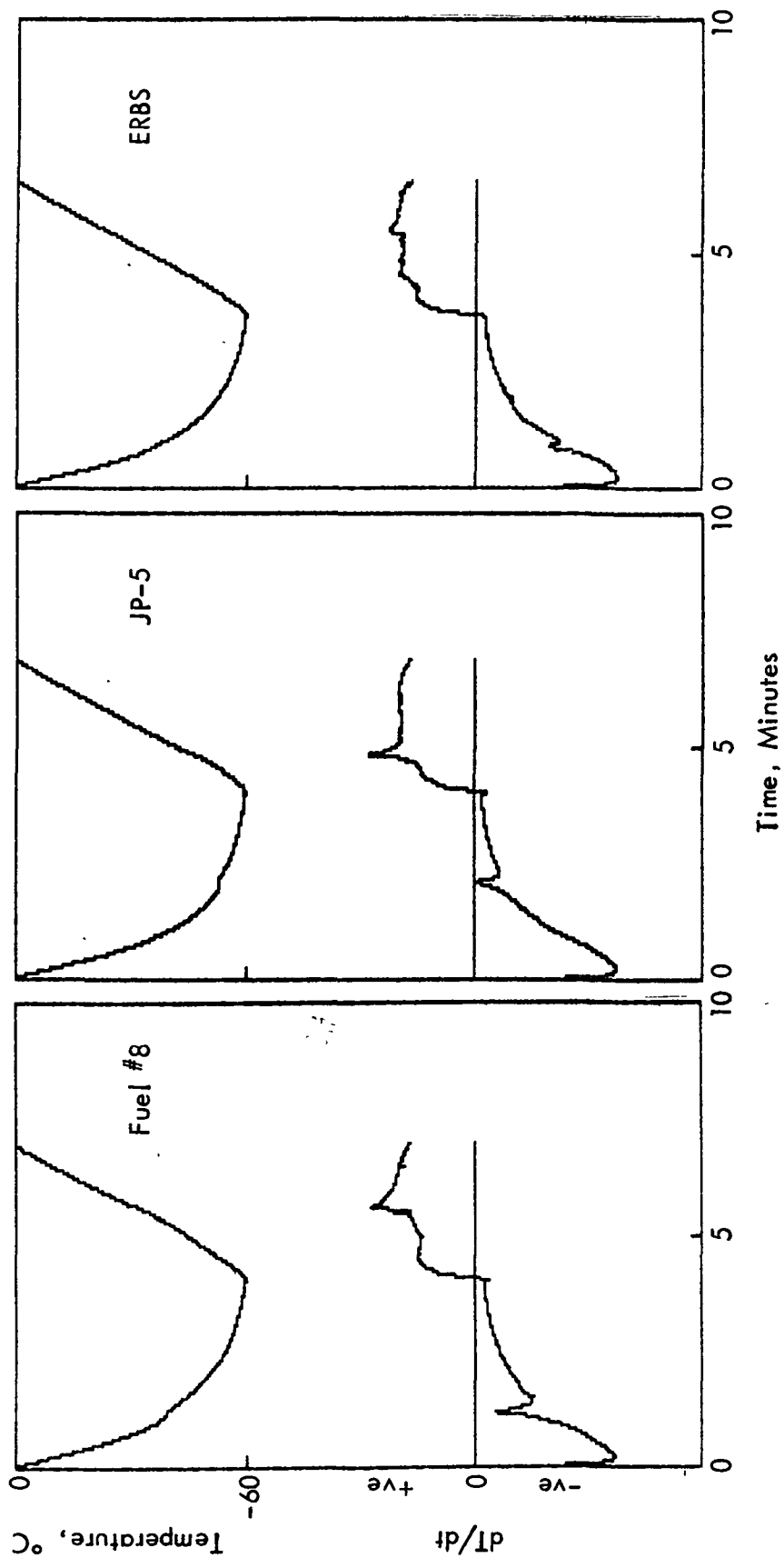


Figure 17 - Experimental T-t and dT/dt-t Plots of Fuel #8, JP-5, and ERBS

## V. DISCUSSION OF TEST RESULTS

The suitability of the point of inflection method to determine the freezing point of a wide variety of fuels depends principally on the accuracy of the results obtainable using this method. Therefore, for the purpose of studying the accuracy of test results, a comparison of results with those reported by other facilities is appropriate. To do this, we first collected the reported freezing points of the 12 fuels. The NASA project manager provided the values measured at NASA by the DSC method. He also made available the values measured at Rensselaer Polytechnic Institute (RPI) and Catholic University of America, using the ASTM and DSC methods. Table 8 shows the freezing point values for the fuels as reported at various laboratories.

Table 9 summarizes the freezing point values measured at MRI and those reported elsewhere using ASTM and DSC methods. Three values are shown under the column "MRI Values," two of them reflecting the values measured at the peak and valley of the  $dT/dt$  curve and the other reflecting the average values measured between the peak and the valley. As mentioned earlier, all the fuels exhibited a clear, identifiable peak. Therefore the results obtained using the sample temperature at peak are highly reliable. However, as shown in Chapter II, a point similar to the peak of a DTA signal does not correspond to the peak in the  $dT/dt$  signal. Therefore, one would expect that the temperature measured at the peak of the  $dT/dt$  curve would be higher than the sample's freezing point. The MRI values measured at the peak of the  $dT/dt$  curve are about  $2^{\circ}\text{C}$  higher than the reported values, with the difference from the ASTM data averaging  $2.2^{\circ}\text{C}$  and from the DSC  $1.8^{\circ}\text{C}$ . Since the values measured at the peak are highly reliable, but carry a finite difference, it is possible to determine the freezing point of aviation fuel by measuring the temperature at the peak and then subtracting a constant temperature from the measured value.

Figure 18 shows the MRI values obtained at the peak and corrected by  $2.0^{\circ}\text{C}$  compared with those obtained by the DSC and ASTM methods. It can be seen that after the correction is made on the values predicted at the peak, there is good agreement with the MRI predicted values and the ASTM and DSC values, as indicated by the 45-degree line representing perfect agreement. With the correction applied, the average absolute difference is  $0.7^{\circ}\text{C}$ , and the standard deviation is  $0.8^{\circ}\text{C}$ . It is possible to further improve the correlation by applying separate corrections to the ASTM data and the DSC data, but the improvement is so small that it is probably not warranted.

In all of the freezing point tests, we also attempted to identify the location of the valley preceding the peak in the  $dT/dt$  curve. When the plots were examined it was found that some fuels do not exhibit a clearly identifiable valley. However, with some logic supplied to the computer, the location of the valley and the sample temperature at this location were obtainable in all the tests. The MRI results reported under the column "valley" in Table 9 show these values. Even though the valleys can be located from the digital data, sometimes they are so shallow that they cannot

TABLE 8  
REPORTED VALUES OF FREEZING POINT  
(Freezing Point, °C)

Fuel	ASTM D-2386			DSC			
	CU <sup>a</sup>	RPI <sup>b</sup>	Average	CU <sup>a</sup>	RPI <sup>b</sup>	NASA	Average <sup>c</sup>
LFP-1	-40.7	-41.0	-40.9	-39.7	-40.2	-38.5	-39.2
LFP-3	-16.5	-16.6	-16.6	-16.8	-	-17.7	-17.3
LFP-4	-13.0	-12.6	-12.8	-12.5	-11.8	-13.7	-12.9
LFP-6	-27.9	-29.1	-28.5	-28.6	-26.3	-27.2	-27.3
LFP-7	-10.3	-12.6	-11.5	-12.8	-12.1	-13.0	-12.7
LFP-8	-49.8	-49.3	-49.6	-51.0	-	-51.6	-51.3
LFP-9	-45.1	-45.1	-45.1	-44.0	-43.6	-43.0	-43.4
LFP-14	-	-33.1	-33.1	-	-	-33.6	-33.6
Fuel #7	-27.6	-27.9	-27.8	-28.7	-28.7	-26.8	-27.8
Fuel #8	-33.3	-34.6	-34.0	-32.7	-31.4	-31.8	-31.9
JP-5	-	-49.4	-49.4	-	-47.7	-47.5	-47.6
ERBS	-	-24.6	-24.6	-	-22.8	-23.0	-22.9

<sup>a</sup> Values obtained at Catholic University by Professor Moynihan.

<sup>b</sup> Values obtained at Rensselaer Polytechnic Institute by Professor Moynihan.

<sup>c</sup> Average was determined using the following weight factors: CU-1, RPI-1, NASA-2 for LFP-1, LFP-4, LFP-6, LFP-7, LFP-9, Fuel #7, and Fuel #8; CU-1, NASA-1 for LFP-3 and LFP-8; RPI-1, NASA-1 for JP-5 and ERBS.



TABLE 9

TEST RESULTS AND COMPARISON  
(Freezing Point in °C)

<u>Fuel</u>	<u>Reported Values</u>		<u>MRI Values</u>		
	<u>ASTM</u>	<u>DSC</u>	<u>Peak</u>	<u>Valley</u>	<u>Average</u>
LFP-1	-40.5	-39.2	-38.3	-40.9	-39.6
LFP-3	-16.6	-17.3	-15.7	-17.7	-16.7
LFP-4	-12.8	-12.9	-11.2	-12.7	-11.9
LFP-6	-28.5	-27.3	-25.7	-27.0	-26.4
LFP-7	-11.5	-12.7	-10.2	-14.7	-12.4
LFP-8	-49.6	-51.3	-48.4	-51.5	-49.9
LFP-9	-45.1	-43.4	-41.4	-43.7	-42.6
LFP-14	-33.1	-33.6	-30.8	-34.3	-32.6
Fuel #7	-27.8	-27.8	-26.2	-32.0	-29.1
Fuel #8	-34.0	-31.9	-31.4	-33.1	-32.3
JP-5	-49.4	-47.6	-45.8	-48.4	-47.1
ERBS	-24.6	-22.9	-21.7	-22.5	-22.1

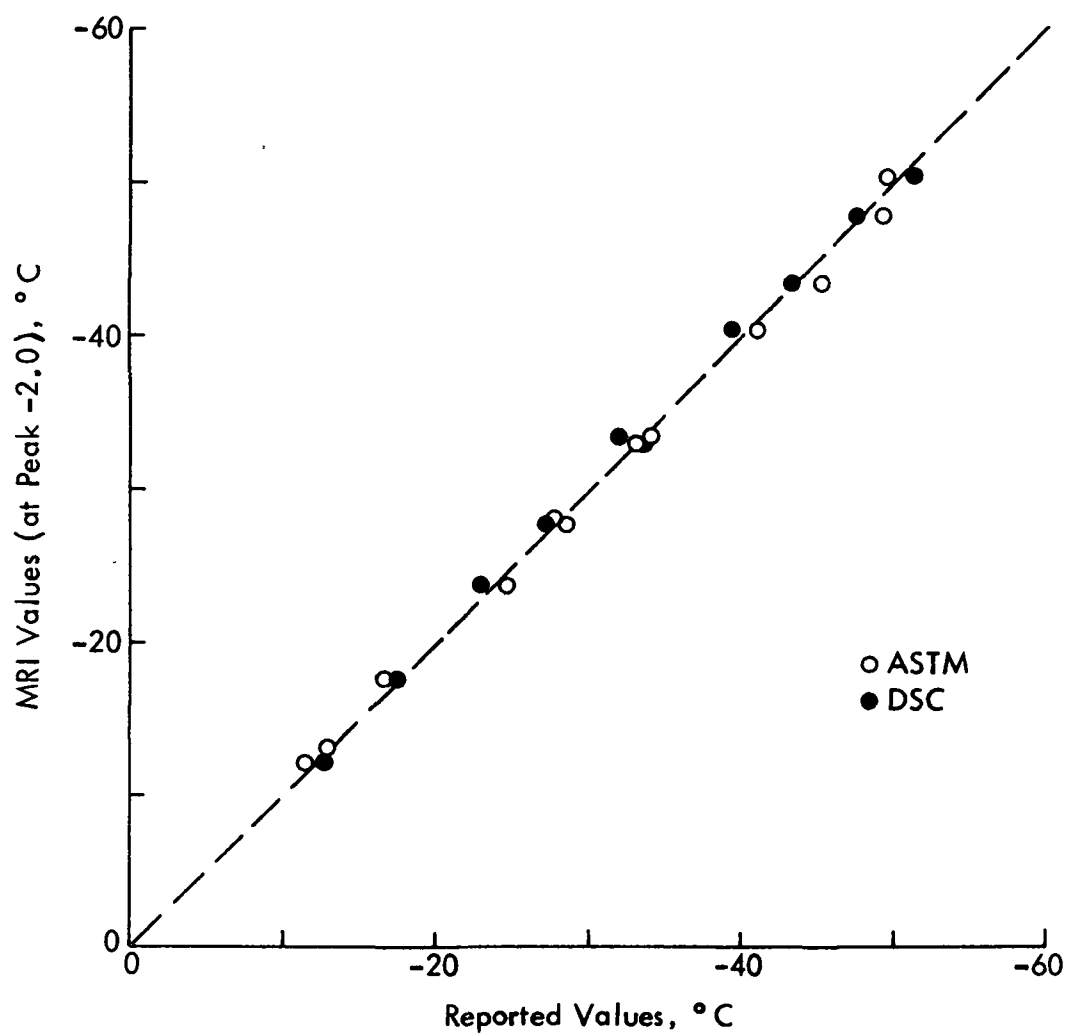


Figure 18 - Comparison of MRI Values (Peak - 2.0°C) Versus Reported Values

be seen in the plots. Because of this we decided to use the values obtained at the valley very cautiously. We believe that the values measured at the valley are not as reliable as those measured at the peak.

The purpose of finding the temperature at the valley is to examine whether or not the average between the temperature at the peak and the valley correlates with the reported values of the freezing point. Table 9 also includes these average values. As was discussed in the basic analysis chapter, one can expect that the average temperature may closely represent the temperature at the peak of a DTA-generated  $\Delta T$  curve and therefore the freezing point.

Figure 19 shows the comparison of the MRI values obtained by averaging the peak and valley temperatures with those obtained by the DSC and ASTM methods. The overall agreement is good, with the average absolute difference being  $1.0^{\circ}\text{C}$ , and the standard deviation being  $1.2^{\circ}\text{C}$ . Separately, the DSC results had an average absolute difference of  $0.8^{\circ}\text{C}$  (standard deviation  $0.9^{\circ}\text{C}$ ), and the ASTM an average absolute difference of  $1.3^{\circ}\text{C}$  (standard deviation  $1.5^{\circ}\text{C}$ ). The largest difference in the ASTM data was  $2.5^{\circ}\text{C}$  which is within the reproducibility of the ASTM method.

The results using the midpoint between the valley and the peak are not as good as those using the peak with a correction applied. It is possible to improve the correlation by the selection of a point, other than the midpoint, which best fits the data. However, if an empiricism is to be used, it would be better to select a method which involves only the peak value, because the peak value is simpler to obtain and more reliable. Therefore, the use of the peak value minus a constant  $2^{\circ}\text{C}$  correction appears to be the preferred method.

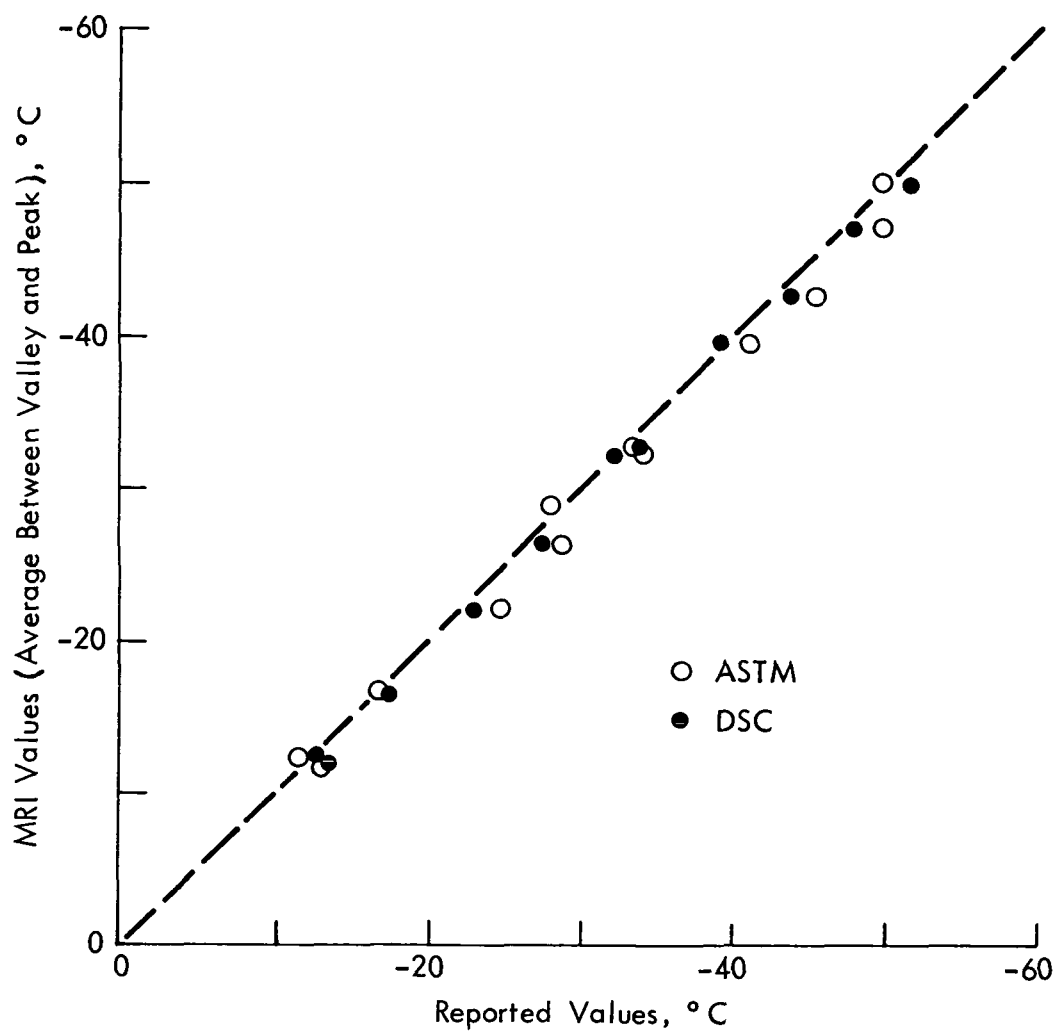


Figure 19 - Comparison of MRI Values (Average Between Valley and Peak) Versus Reported Values

## VI. CONCLUSIONS AND RECOMMENDATIONS

This chapter contains the conclusions and recommendations based on the results of this study. The conclusions are presented in Section A and the recommendations in Section B.

### A. Conclusions

1. The freezing point apparatus developed previously was modified to provide controlled cooling and rewarming rates. In the modified apparatus, temperatures as low as  $-60^{\circ}\text{C}$  are achievable and, if necessary, the minimum temperature can be held for a predetermined period at the end of cooling.

2. The concept used to identify the freezing point is referred to as the "point of inflection method." In this method a point of inflection in the temperature-time curve exhibited by the sample at the end of melting is identified, and the sample temperature at this time corresponds to the ASTM D-2386 freezing point.

3. The rate of cooling and the hold period at the end of cooling have insignificant effects on the measured freezing point. However, the rate of rewarming has a significant effect and therefore needs to be optimized. For aviation and diesel fuels, and the sample size used in the test apparatus, a rewarming rate of approximately  $22^{\circ}\text{C}/\text{min}$  appears to be optimum. At this rewarming rate all the fuels, including weak-peak-exhibiting fuels, exhibit an identifiable point of inflection.

4. The optimum test procedure calls for an uncontrolled cooling to either  $-60^{\circ}\text{C}$  or  $10-15^{\circ}\text{C}$  below the cloud point, whichever is lower, followed by a controlled rewarming at about  $22^{\circ}\text{C}/\text{min}$ . No hold time is necessary.

5. Using the modified apparatus the freezing point can be measured rapidly. The time required to complete a single test is as little as 5 to 7 min, and in no case exceeds 10 min.

6. Freezing points measured by the point of inflection method using the peak of the temperature derivative versus time curve average  $2^{\circ}\text{C}$  high compared to corresponding ASTM D-2386 and DSC measurements. An improvement is made by using the midpoint from the bottom of the curve ("the valley") to the peak. However, it is considerably more difficult and less reliable to identify the valley rather than the peak. The recommended procedure for the freezing point is to correct the temperature at the peak by subtracting  $2^{\circ}\text{C}$ .

### B. Recommendations

Based on the results of this study, a number of suggestions can be made to assist in the design of a portable instrument to improve performance and to incorporate additional capabilities. These are discussed in the following paragraphs.

1. In the current study the freezing point apparatus was modified by adding suitable electronic controls to provide constant cooling and rewarming rates. With further minor modification, the apparatus can be configured to provide a constant heat flow rate during cooling and rewarming. The heat flow rate equation is given by:

$$\dot{Q} = mC_p (dT/dt) \quad (4)$$

where  $\dot{Q}$  = heat flow rate, J/min

$m$  = mass of sample in holder, g

$C_p$  = specific heat of the sample, J/g/°C

$dT/dt$  = rate of change of temperature, °C/min

During freezing (while cooling) and melting (while rewarming) processes,  $C_p$  represents the total specific heat which includes both sensible heat and latent heat. In the present apparatus, the value of  $dT/dt$  can be measured as a function of sample temperature. With the proposed modification, the value of  $\dot{Q}$  can be made constant in time; the value of  $\dot{Q}$  can also be determined accurately. Therefore, it would be possible to determine  $C_p$  as a function of temperature during cooling and rewarming which involve freezing and melting processes. For any substance, it is well-known that the value of specific heat  $C_p$  is necessary for modeling the heat transfer and for determining the transient thermal response of the substance. In an aircraft wing tank, this information is useful to determine the temperature distribution within the fuel when the air craft is flying for several hours. With the proposed simple modification,  $C_p$  can be determined for a variety of substances including aviation fuels and this information will be a significant contribution to the researchers in several areas.

2. As can be seen from the text of this report, the developed freezing point apparatus is simple both in construction and in operation. It appears that the apparatus can further be simplified to increase its portability advantages. For example, if the process of finding the temperature derivative ( $dT/dt$ ) by analog differentiation is switched to numerical differentiation, then the analog differentiator, a component presently necessary, can completely be eliminated. To examine this possibility, it may be necessary to increase the rate at which the data are scanned. As of now, the data are scanned at the rate of 2 sets/sec. Scanning rates as high as 20 per second will enable the incorporation of suitable curve-smoothing techniques into the software program. High scanning rates permit the use of curve-smoothing techniques without destroying the salient thermal events present in the temperature signal. A smoothed temperature-time curve is numerically differentiable without significant unstable solutions built into it. A high resolution A/D converter may also be necessary. Our present converter has 12 bits of resolution; we recommend replacing it by a 16 bit resolution converter. In addition to the simplicity advantages, it is possible to get more accurate values of freezing point by this arrangement.

3. In the current program activities, we focused on optimizing the cooling and rewarming rates to determine the freezing point accurately. As per the ASTM method, the freezing point was measured using the data obtained during rewarming. The data collected during cooling were not used. However, as can be seen from the  $dT/dt$  curves a peak, and sometimes a valley, are formed during the cooling process. The temperatures measurable at these points may correspond to what is called the cloud point (ASTM D-2500). It would be possible to include the optimization of cooling rates to determine the cloud point accurately. This work would form a basis to develop a combined cloud point and freezing point apparatus, where both could be determined well within 10 min in a single test. Any cooling rate that may be found optimum to determine the cloud point, will not have influence on the freezing point determination, since we have shown that the various cooling rates have insignificant effects on the measured freezing point.

4. A possible limitation to the commercial application of the point of inflection method to determine the freezing point is the correction required to account for the temperature gradients in the fuel. We have shown that an adjustment of about  $2^{\circ}\text{C}$  is necessary to match the proposed method results with the reported values. In this regard, it would be desirable to investigate various methods to eliminate the temperature gradients. One could examine the possibility of reducing the size of the thermoelectric modules and also the size of the sample. As of now, the face of the TE module in contact with the sample holder has dimensions of 30 x 30 mm square. These should be replaced by a TE module having face dimensions of 10 mm or less. The sample holder can also be sized accordingly. The sample mass required can thus be reduced by a factor of 10 or so. By further reducing the thickness of sample holder, the sample size can be reduced significantly. A small TE module would result in two smaller ice-water boxes. Thermal equilibrium will be more closely approached, and possibly no correction will be required with the proposed small-size apparatus.

**Page intentionally left blank**

**Page intentionally left blank**



## APPENDIX A

### Heat Transfer Equations and Solution for the Rewarming Process

Let a test sample previously cooled to a temperature  $T_i$  and existing in the solid phase be rewarmed in a thermoelectric cooler.<sup>i</sup> Let also the highest temperature that the sample would attain during rewarming be  $T_o$ . The value of  $T_o$  depends on the current flow to the TE modules. The sample attains  $T_o$  after a very long time ( $t \rightarrow \infty$ ). Then  $T_o$  represents the effective temperature of the surroundings causing heat to flow into the sample. Let  $R$  be the thermal resistance to heat flow between the surroundings and the test sample. The heat transfer equation for this rewarming process is given by:

$$C \frac{dT}{dt} + \frac{T - T_o}{R} = 0 \quad (A-1)$$

where  $C$  is the heat capacity of the test sample (product of the mass of sample and its specific heat) and  $T$  is the sample temperature.  $C$  accounts for sensible heat when the sample is in solid phase or liquid phase and it accounts for both latent and sensible heat when the sample is two phase. For the sake of simplicity, the value of  $C$  is assumed to be constant but it could be a different constant for different regimes such as  $C = C_1$  during solid phase,  $C = C_2$  during two phase, and  $C = C_3$  during liquid phase. In general  $C_2$  is greater than  $C_1$  or  $C_3$  since  $C_2$  includes the latent heat. For pure species  $C_2$  approaches infinity, since the latent heat is absorbed with no rise in temperature.

### Solution for Solid Phase Regime

The solution of the governing equation (A-1) subjecting to the initial condition of  $T = T_i$  at  $t = 0$  is given by:

$$T = T_o + (T_i - T_o) \exp(-t/RC_1) \quad (A-2)$$

If  $T_f$  is the sample temperature when the solid begins to melt, then the time  $t_f$  at which this would occur can be determined from (A-2) and is given by:

$$t_f = RC_1 \ln [(T_o - T_i)/(T_o - T_f)] \quad (A-3)$$

Equation (A-2) is valid for  $0 < t < t_f$ .

### Solution for Two-Phase Regime

The solution of the governing equation (A-1) for the two-phase regime must be obtained separately for mixtures and pure species.

For a multicomponent mixture,  $C = C_2$  and is finite. The solution of equation (A-1) subjecting to the condition of  $T = T_f$  at  $t = t_f$  is given by:

$$T = T_o + (T_f - T_o) \exp [(t_f - t)/RC_2] \quad (A-4)$$

The value of  $t_f$  required in this equation is known from equation (A-3). If  $T_m$  is the sample temperature when the melting is just complete, then the time at which this would occur  $t_m$  can be determined from (A-4) and is given by:

$$t_m = t_f + RC_2 \ln [(T_o - T_f)/(T_o - T_m)] \quad (A-5)$$

Equation (A-4) is valid for  $t_f \leq t \leq t_m$ .

For a pure species, the value of  $C$  approaches infinity in the two-phase regime. Substituting  $C_2 = \infty$  in equation (A-4), one gets  $T = T_f$  for this regime. This is well-known for pure species. Therefore, we can write  $T = T_f$ . To determine the value of  $t_m$ , the time at which the melting is just complete, the value of the latent heat  $L$  must be known. The heat flow rate is  $(T - T_f)/R$  and therefore the time required to release a total latent heat of  $Q_L$  would be  $RL/(T_o - T_f)$ . Hence we get:

$$t_m = t_f + RL/(T_o - T_f) \quad (A-6)$$

### Solution for Liquid Phase Regime

The solution of the governing equation (A-1) subjecting to the condition of  $T = T_m$  can be written as:

$$T = T_o + (T_m - T_o) \exp [(t_m - t)/RC_3] \quad (A-7)$$

The value of  $t$  required to be used in this equation is obtainable from equation (A-5) or (A-6). Equation (A-7) is valid for  $t > t_m$ .

### Temperature Derivatives

From the temperature histories derived for the three regimes, it is possible to determine the first derivatives of temperature ( $dT/dt$ ) which are given below.

(i) Solid phase ( $t \leq t_f$ )

$$\frac{dT}{dt} = \frac{T_o - T_i}{RC_1} \exp\left(\frac{-t}{RC_1}\right) \quad (A-8)$$

(ii) Two phase ( $t_f \leq t \leq t_m$ )

$$\begin{aligned} \frac{dT}{dt} &= \frac{T_o - T_f}{RC_2} \exp\left(\frac{t_f - t}{RC_2}\right) && \text{.... mixtures} \\ \frac{dT}{dt} &= 0 && \text{.... pure species} \end{aligned} \quad (A-9)$$

(iii) Liquid phase ( $t \geq t_m$ )

$$\frac{dT}{dt} = \frac{T_o - T_m}{RC_3} \exp\left(\frac{t_m - t}{RC_3}\right) \quad (A-10)$$

For the purpose of illustrating the existence of the point of inflection at the freezing point (i.e., at  $t = t_m$ ),  $T$  versus  $t$  and  $dT/dt$  versus  $t$  generated using the equations listed above for (i) a pure species and (ii) a mixture. The following values were used to generate these plots.

	<u>Pure Species</u>	<u>Mixture</u>
$T_i$ ( $^{\circ}\text{C}$ )	-60	-60
$T_o$ ( $^{\circ}\text{C}$ )	20	20
$R$ ( $^{\circ}\text{C}/\text{W}$ )	12	12
$C_1$ ( $\text{J}/^{\circ}\text{C}$ )	7	7
$C_2$ ( $\text{J}/^{\circ}\text{C}$ )	-	14
$C_3$ ( $\text{J}/^{\circ}\text{C}$ )	7	7
$T_f$ ( $^{\circ}\text{C}$ )	-20	-40
$T_m$ ( $^{\circ}\text{C}$ )	-20	-20
$L$ ( $\text{J}$ )	140	-

The plots are shown in Figure (20). It can be seen from these plots that the points of inflection do exist at the end of melting process. Therefore, the temperature measured here would represent the freezing point. For the purpose of comparison, the  $T$  versus  $t$  and  $dT/dt$  versus  $t$  plots are also shown in dotted lines for a nonfreezing substance having  $C_1 = C_2 = C_3 = 7 \text{ J}/^{\circ}\text{C}$ .

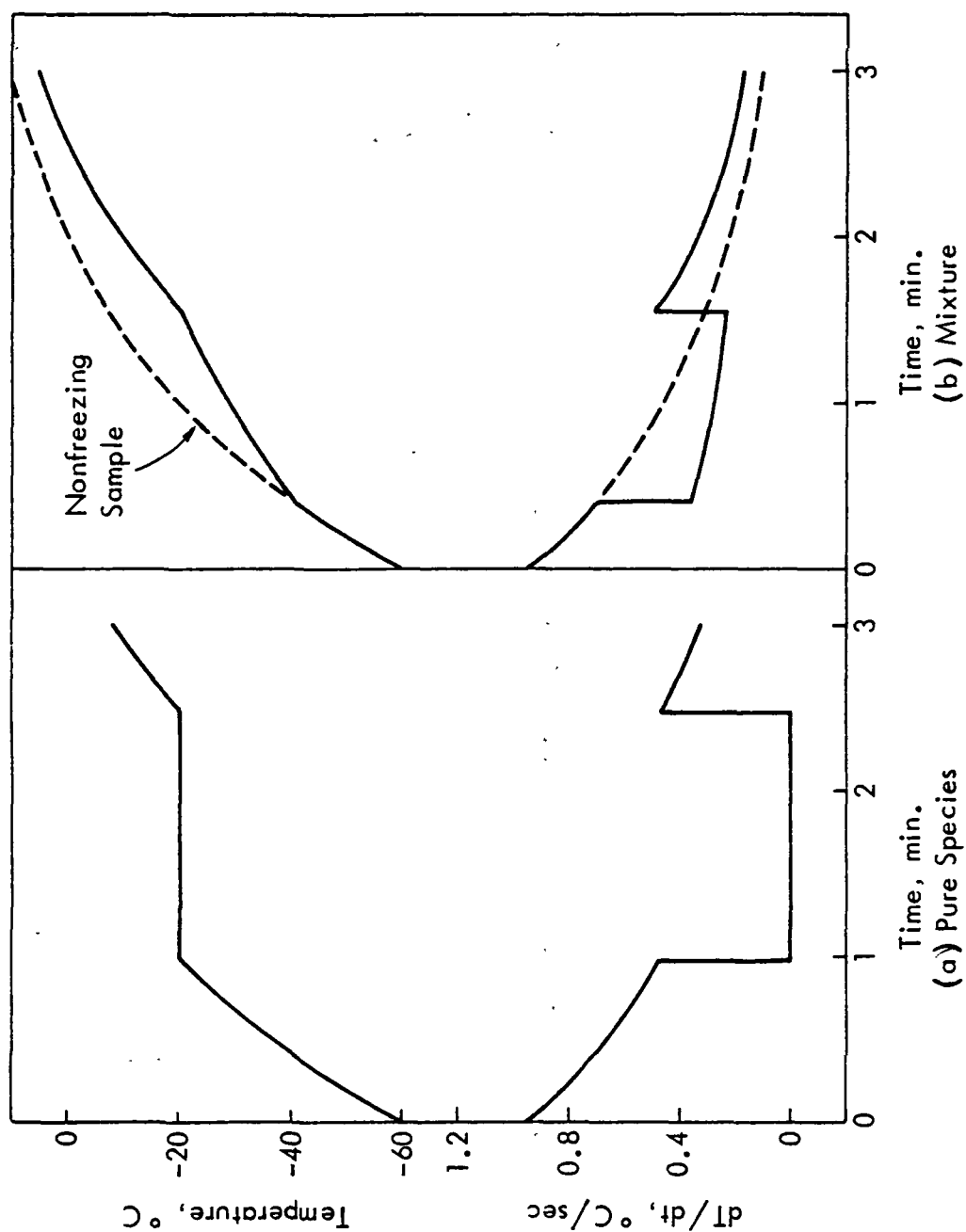


Figure 20. Theoretical T-t and  $dT/dt$ -t plots

## REFERENCES

1. Mathiprakasam, B. "Evaluation of Methods for Rapid Determination of Freezing Point of Aviation Fuels." NASA CR-167981, September 1982, NTIS Report No. N83-10207/9.
2. Daniels, T. "Techniques Based on Changes in Thermal Properties." Thermal Analysis. Kogan Page Limited, London, 1973:73-135.
3. Gray, A. P. "A Simply Generalized Theory for the Analysis of Dynamic Thermal Measurement." Analytical Chemistry, Vol. I, 1968:209-218.
4. Moynihan, C. T., M. R. Shahriari, and T. Bardakci. "Thermal Analysis of Melting and Freezing of Jet and Diesel Fuels." Thermochimica Acta, Vol. 52, 1982:131-141.

1 Report No NASA CR 168305	2 Government Accession No	3 Recipient's Catalog No	
4 Title and Subtitle  EXPERIMENTAL RESULTS FOR THE RAPID DETERMINATION OF THE FREEZING POINT OF FUELS		5 Report Date February 1984	
		6. Performing Organization Code	
7 Author(s)  B. Mathiprakasam		8 Performing Organization Report No 7014-S	
9 Performing Organization Name and Address Midwest Research Institute 425 Volker Boulevard Kansas City, Missouri 64110		10 Work Unit No.	
		11 Contract or Grant No. NAS 3-22543	
		13. Type of Report and Period Covered Contractor Report	
12 Sponsoring Agency Name and Address National Aeronautics and Space Administration Washington, D.C. 20546		14. Sponsoring Agency Code 505-31-42	
15 Supplementary Notes  Project Manager, Roger A. Svehla, Aerothermodynamics and Fuels Division NASA Lewis Research Center, Cleveland, Ohio			
16 Abstract  This is a continuation of an investigation of methods for the rapid determination of the freezing point of fuels. In the preceding work a search and evaluation of possible techniques resulted in two methods for further study. The two methods selected were an optical method, which detected the change in light transmission from the disappearance of solid particles in the melted fuel, and a differential thermal analysis (DTA) method, which sensed the latent heat of fusion. A laboratory apparatus was fabricated to test the two methods. Cooling was done by thermoelectric modules using an ice-water bath as a heat sink. The DTA method was later modified to eliminate the reference fuel. The data from the sample were digitized and a point of inflection, which corresponds to the ASTM D-2386 freezing point (final melting point), was identified from the derivative. This modified method was chosen for further testing.  In the present work, the apparatus was modified to cool the fuel to -60°C and controls were added for maintaining constant cooling rate, rewarming rate, and hold time at minimum temperature. A parametric series of tests were run for twelve (12) fuels with freezing points from -10°C to -50°C, varying cooling rate, rewarming rate, and hold time. Based on the results, an optimum test procedure was established. The results showed good agreement with ASTM D-2386 freezing point and differential scanning calorimetry results.			
17 Key Words (Suggested by Author(s))  Aircraft Fuels Fuel Freezing Point		18. Distribution Statement  Unclassified-Unlimited STAR Category 28	
19 Security Classif. (of this report) Unclassified	20 Security Classif (of this page) Unclassified	21. No. of Pages 61	22. Price*